Monthly Notices of the ROYAL ASTRONOMICAL SOCIETY

MNRAS **527,** 9303–9321 (2024)
Advance Access publication 2023 November 8

https://doi.org/10.1093/mnras/stad3342

Revisiting the classics: on the evolutionary origin of the 'Fe II' and 'He/N' spectral classes of novae

E. Aydi [1★†] L. Chomiuk [1★] J. Strader,[1] K. V. Sokolovsky [2,3] R. E. Williams,[4,5] D. A. H. Buckley [6,7] A. Ederoclite [8] L. Izzo [9,10] R. Kyer [1] J. D. Linford [11] A. Kniazev [3,6,12,13] B. D. Metzger [14,15] J. Mikołajewska [16] P. Molaro [17,18] I. Molina,[1] K. Mukai [19,20] U. Munari,[21] M. Orio [22,23] T. Panurach [1,24] B. J. Shappee [25] K. J. Shen [26] J. L. Sokoloski,[27] R. Urquhart[1] and F. M. Walter [28]

Affiliations are listed at the end of the paper

Accepted 2023 October 25. Received 2023 October 25; in original form 2023 September 14

ABSTRACT

The optical spectra of novae are characterized by emission lines from the hydrogen Balmer series and either Fe II or He/N, leading to their traditional classification into two spectral classes: 'Fe II' and 'He/N'. For decades, the origins of these spectral features were discussed in the literature in the contexts of different bodies of gas or changes in the opacity of the ejecta, particularly associated with studies by R. E. Williams and S. N. Shore. Here, we revisit these major studies with dedicated, modern data sets, covering the evolution of several novae from early rise to peak all the way to the nebular phase. Our data confirm previous suggestions in the literature that the 'Fe II' and 'He/N' spectral classes are phases in the spectroscopic evolution of novae driven primarily by changes in the opacity, ionization, and density of the ejecta, and most if not all novae go through at least three spectroscopic phases as their eruptions evolve: an early He/N (phase 1; observed during the early rise to visible peak and characterized by P Cygni lines of He I and N II/III), then an Fe II (phase 2; observed near visible peak and characterized by P Cygni lines of Fe II and O I), and then a later He/N (phase 3; observed during the decline and characterized by emission lines of He I/II, N II/III), before entering the nebular phase. This spectral evolution seems to be ubiquitous across novae, regardless of their speed class; however the duration of each of these phases differs based on the speed class of the nova.

Key words: (*stars:*) novae, cataclysmic variables – (*stars:*) white dwarfs – transients: novae.

1 INTRODUCTION

A classical nova is a thermonuclear eruption occurring in the hydrogen-rich shell formed on the surface of a white dwarf (WD) star accreting material from a nearby stellar companion (for reviews see, e.g. Gallagher & Starrfield 1976; Bode & Evans 2008; Della Valle & Izzo 2020; Chomiuk, Metzger & Shen 2021). The thermonuclear eruption produces an optical transient, where the system brightens by 8 up to 15 magnitudes, reaching naked-eye brightness in some cases.

For decades, nova eruptions were monitored using optical spectroscopy, where emission and absorption lines of a wide diversity of species are observed, characterized by velocities ranging from a few hundreds up to a few thousands km s^{-1} (e.g. McLaughlin 1944; Mclaughlin 1947; Payne-Gaposchkin 1957; Aydi et al. 2020b). Typically, the strongest lines in nova spectra are those of the hydrogen Balmer series, followed by either low-ionization Fe II lines particularly of the (42, 48, and 49) multiplets, or high-excitation He I, He II, N II, and N III lines. These distinct species that dominate nova spectra near the peak brightness led to classifying novae under two main spectral classes: 'Fe II' and 'He/N' novae (Williams 1992, 2012). In addition to showing different species of emission/absorption lines, the classes are characterized by different ejecta velocities, with Fe II novae showing slower ejecta velocities (FWHM $<$ 2500 km s^{-1}) compared to He/N novae (FWHM $>$ 2500 km s^{-1}) and spectral lines profiles (Fe II novae tend to show more P Cygni line profiles while He/N novae show broad, flat-topped emission lines; Williams 1992).

Mainly, the origin of these spectral features have been attributed to different bodies of gases (e.g. Williams et al. 2008; Williams 2012) or changes in the condition of the nova ejecta (e.g. Shore 2012, 2013, 2014; Mason et al. 2018). Williams (2012) suggested that the Fe II spectra possibly have origin in stripped material from the companion star residing around the binary system, while the He/N spectra originate in ejected material from the surface of the WD. However, Shore (2014) suggested that the Fe II and He/N spectra are defined by the opacity and ionization state of the ejecta and therefore Fe II novae are observed at a stage where the ejecta are optically thick, while He/N novae are observed after peak at a stage where the ejecta are optically thin (or even completely ionized).

While novae were assigned specific spectral classes as Fe II or He/N based on their spectra observed after optical peak, Williams (2012) suggested that if dedicated spectroscopic follow-up were available, some if not all novae might show features of both classes

★ E-mail: aydielia@msu.edu (EA); Chomiukl@msu.edu (LC)
† Elias Aydi - NFHP Hubble Fellow

simultaneously or evolve from one class to another, and dubbed them as 'hybrid' novae. Shore (2012, 2014) also suggested that the same nova could show an evolution from one class to another depending on the conditions within the novae ejecta (i.e. changes in opacity, ionization, and density). This hybrid evolution has been observed and discussed in the literature for a few novae, for example the 2011 eruption of T Pyx (Shore et al. 2011; Ederoclite 2014; Surina et al. 2014; Arai et al. 2015) and V5558 Sgr (Tanaka et al. 2011b).

We have entered a new era of all-sky surveys that monitor the sky nightly, facilitating the discovery of novae at the earliest stages of eruption. These now-routine early discoveries of novae, combined with rapid spectroscopic follow-up by professional astronomers and citizen scientists allow us to gather comprehensive spectroscopic data sets for a substantial sample of novae, tracking their eruptions from start to end. Backed by these spectroscopic data sets, we revisit the above-mentioned pioneering studies, with the aims of establishing a unifying picture of nova spectroscopic evolution and drawing new insights into the origin of the Fe II and He/N spectral classes. In Section 2, we discuss our nova sample and the observations and data reduction. In Section 3 we present the results, including the spectroscopic evolution of the novae in the sample. These results are further discussed in Section 4, while our conclusions are presented in Section 5.

2 OBSERVATIONS AND DATA REDUCTION

Our main sample consists of six well-observed novae, namely T Pyx (2011), V339 Del (2013), V659 Sct (2019), V1405 Cas (2021), V606 Vul (2021), and *Gaia*22alz (2022), which all show an analogous spectroscopic evolution throughout their eruptions despite the different time-scales of their eruptions. These novae were selected based on the availability of dedicated spectroscopic monitoring throughout the evolution of the nova eruption, from the early rise to peak all the way to the nebular phase. While we are aware that other novae might have comparable dedicated observational follow-up in the literature, we limit our main sample to six novae so we can showcase their evolution clearly in a reasonably compact manuscript. The main sample consists of novae from different speed classes (very fast, fast, slow, and very slow as classified based on the time to decline by two magnitudes from maximum t_2; Payne-Gaposchkin 1957). Selecting novae of different speed classes emphasizes that the proposed spectral evolution is common across fast and slow novae. We also show the early spectral evolution of four additional, supporting cases: two slow novae (V612 Sct 2017 and FM Cir 2018); and two very fast novae (V407 Lup 2016 and U Sco 2022), with the aim of demonstrating the prevalence of the universal spectral evolution we propose in this work, regardless of the speed class of the nova. It is worth noting that all the novae in our sample are known to have dwarf companion stars, with the exception of U Sco, where the companion star might be more evolved, that is, a sub-giant donor (Schaefer 1990). In Table 1, we list the details of all the novae in our sample.

The spectra presented in this paper derive from a variety of facilities and sources, including both professional observatories and contributions from citizen scientists. Here we provide a brief summary of the facilities and instruments utilized for spectroscopic observations, while the detailed observation logs for each nova may be found in Appendix Tables A1, A2, A3, A4, A5, A6, A7, A8, A9, and A10.

(i) A fraction of the spectra used in this work were obtained using the Goodman spectrograph (Clemens, Crain & Anderson 2004) on the 4.1-m Southern Astrophysical Research (SOAR) telescope located on Cerro Pachón, Chile. The spectra were reduced and optimally extracted using the APALL package in IRAF (Tody 1986).

(ii) Another fraction of the spectra used in this paper were obtained using the High-Resolution Spectrograph (HRS; Barnes et al. 2008; Bramall et al. 2010, 2012; Crause et al. 2014) and the Robert Stobie Spectrograph (RSS; Burgh et al. 2003; Kobulnicky et al. 2003) mounted on the Southern African Large Telescope (SALT; Buckley, Swart & Meiring 2006; O'Donoghue et al. 2006) in Sutherland, South Africa. The primary reduction of the HRS spectroscopy was conducted using the SALT science pipeline (Crawford et al. 2010), which includes over-scan correction, bias subtraction, and gain correction. The rest of the reduction was done using the MIDAS HRS pipeline described in details in Kniazev, Gvaramadze & Berdnikov (2016); Kniazev et al. (2019).

(iii) We also obtained spectroscopic data using the ESO-VLT 8-m telescope with the Fibre-fed Optical Echelle Spectrograph (FEROS; Kaufer et al. 1999). The spectra were reduced and optimally extracted using the APALL package in IRAF.

(iv) Spectral observations were also gathered with the Asiago 1.22-m + B&C telescope. The spectra were fully reduced and fluxed against nightly standards in IRAF following the procedures detailed in the Zwitter & Munari (2000) cookbook.

(v) We also made use of publicly available data from the Astronomical Ring for Access to Spectroscopy (ARAS; Teyssier 2019). These consists of a combination of low-resolution ($R \approx 1000$) and medium-resolution (up to $R \approx 11\,000$) spectra obtained by citizen scientists.

We also make use of publicly available photometry from the American Association of Variable Stars (AAVSO; Kloppenborg 2023) International Data base and the All-Sky automated survey for Supernovae (ASAS-SN; Shappee et al. 2014). These data consists of CCD and CMOS photometry, mostly in the *V*-band, *g*-band, and unfiltered band with *V* zero-point (*CV*), as well as visual estimates; these measurements are used to build the optical light curves for the novae in our sample (Figs 1, 2, 3, 4, 5, 6, 7, 8, 9, and 10).

Table 1. The nova sample.

Name	$t_0^{(a)}$ (UT date)	$t_{max} - t_0$ (days)	V_{max} (mag)	$t_2^{(b)}$ (days)
Main sample				
T Pyx	2011-04-14.29	28	6.2	50 ± 4
V339 Del	2013-08-14.37	2	4.5	11 ± 2
V659 Sct	2019-09-29.06	2.0	8.3	7 ± 1
V1405 Cas	2021-03-18.42	53	5.1	165 ± 5
V606 Vul	2021-07-16.49	16.5	10.0	87 ± 4
*Gaia*22alz	2022-01-25.02	178	10.8	207 ± 5
Slow novae				
V612 Sct	2017-06-19.50	40	8.4	> 172
FM Cir	2018-01-17.87	25	6.5	120 ± 5
Fast novae				
V407 Lup	2016-09-24.00	1.4	5.6	≤ 2.9
U Sco	2022-06-06.72	0.5	7.7	2 ± 0.5

Notes. [a]t_0 is the discovery date.
[b]t_2 is derived as the time between peak brightness and the last time the nova drops by 2 mag from peak.

3 RESULTS

In this section we present the spectral evolution of all the novae in our sample, dividing them into two groups: the main sample consisting of six novae and the supporting sample (consisting of two slow and

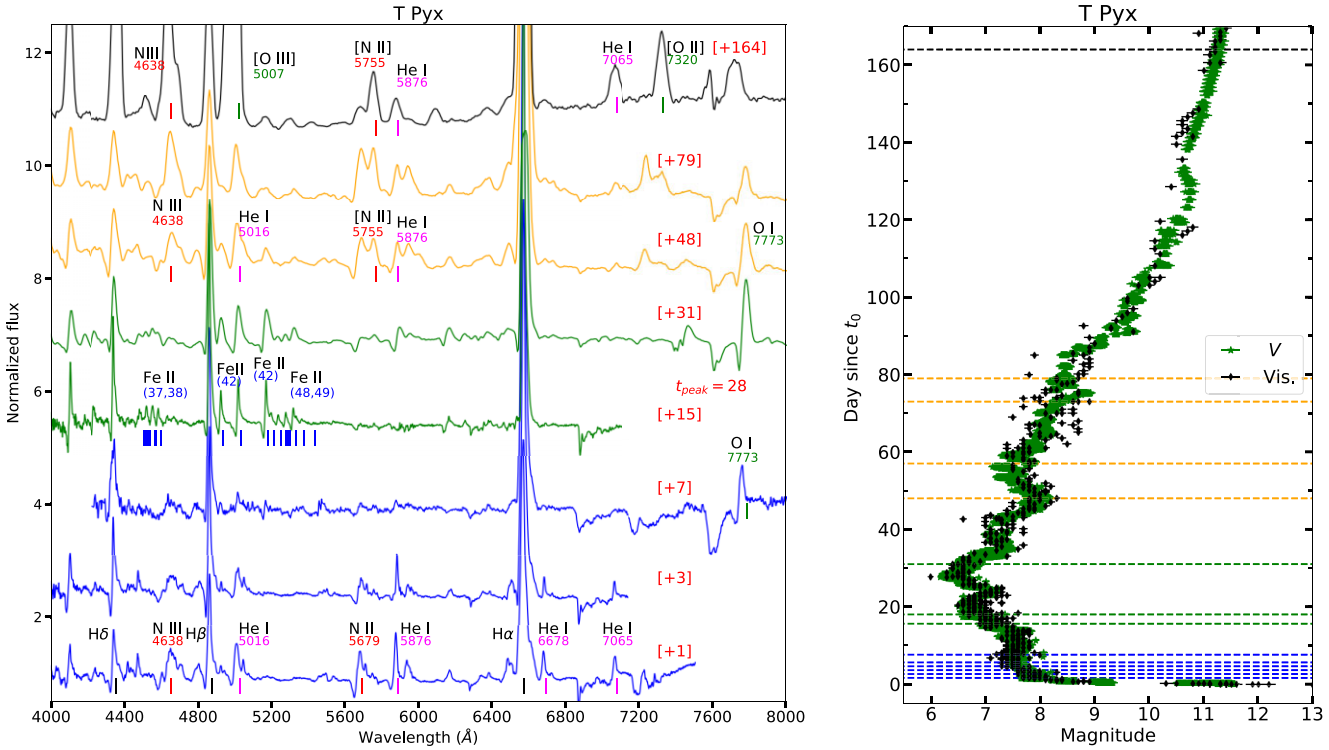

Figure 1. Left: the overall spectroscopic evolution of nova T Pyx representing the different spectral stages: phase 1 (early He/N), highlighted in blue); phase 2 (Fe ii), highlighted in green; phase 3 (late He/N), highlighted in orange; and the nebular phase, highlighted in black. Numbers between brackets are days after t_0. Tick marks are presented under the lines for easier identification and they are color coded based on the line species. Right: the optical light curve of nova T Pyx. The blue, green, orange, and black-dashed lines represent the spectroscopic epochs for when the nova was in phase 1 (early He/N), phase 2 (Fe II), phase 3 (late He/N), and the nebular phase, respectively.

two very fast novae). Here we present the spectroscopic evolution of our nova sample illustrated by selected spectroscopic epochs, while the complete spectroscopic evolution are presented in supplementary online material.

3.1 The main sample

Our main sample consists of six well-observed novae, which show comparable spectroscopic evolution, evolving through at least three distinct phases before they reach the nebular phase. The phases described below are as follow

Early He/N (1) ⟶ FeII (2) ⟶ Late He/N (3).

Below we describe the spectroscopic evolution of each nova in our main sample.

Nova T Pyx (2011): The 2011 eruption of the recurrent Galactic nova T Pyxidis was discovered by M. Linnolt on 2011 April 14.29 UT (HJD 2455665.79; which will be considered as t_0 for this nova; see Schaefer et al. 2013 for more details). Surina et al. (2014) and Arai et al. (2015) presented detailed spectrophotometric studies of the 2011 eruption of T Pyx, focusing on the changes in the spectra and the development of the absorption/emission lines.

In Fig. 1 we present the optical light curve of the nova, which belongs to a moderately fast speed class ($t_2 = 50$ d). It took 28 d for the nova to reach optical peak from the time of discovery. Spectroscopic monitoring starting from day 1.6 all the way to day 164 shows that the nova goes through three phases before it enters the nebular phase. These phases are plotted in Fig. 1, where the spectra are highlighted in different colors for clarity. The spectroscopic evolution consists of: phase 1, highlighted in blue, when the spectra are dominated by P Cygni profiles of Balmer, He I, and N II, and N III, lasting till day 8 after t_0. This phase, covers the early rise to visible peak; phase 2, highlighted in green, when the spectra are dominated by P Cygni profiles or emission lines of Balmer and Fe II and covering the late rise and early decline from visible peak (between days 15 and 40); phase 3, highlighted in orange, when the spectra are again dominated by high-excitation lines of He I, He II, N II, N III, along with Balmer lines. For T Pyx, this phase extends from day 40 until the nova enters the nebular phase around day 150. As the nova enters the nebular phase (highlighted in black in Fig. 1), nebular forbidden lines of singly and doubly ionized oxygen emerge and eventually high-ionization emission lines of forbidden Fe. A detailed spectroscopic evolution of T Pyx, including more spectral epochs is available in the online supplementary material.

Nova V339 Del: The fast nova V339 Del was discovered by Koichi Itagaki on 2013 Aug 14.584 UT at a visual magnitude of around 6.8 (Nakano et al. 2013). Pre-discovery observations of the nova show that the eruption had started as early as 2013 August 14.37 (HJD 2456518.90 $= t_0$; Wren et al. 2013). The overall spectroscopic evolution of the nova and its optical light curve are presented in Fig. 2. The nova evolution was fast, with $t_2 = 11$ d. It also took just 2 d for the nova to reach optical peak from the time of discovery. The first spectrum obtained for the nova, less than a day after discovery, shows P Cygni lines of H Balmer and He I, with relatively weak Fe II P Cygni lines. In the following epochs, taken over the following days, the He I lines weakened, while the Fe II lines became more prominent. Due to the presence of weak Fe II lines in the first epoch, we suggest that this epoch was obtained during a relatively rapid (a few hours

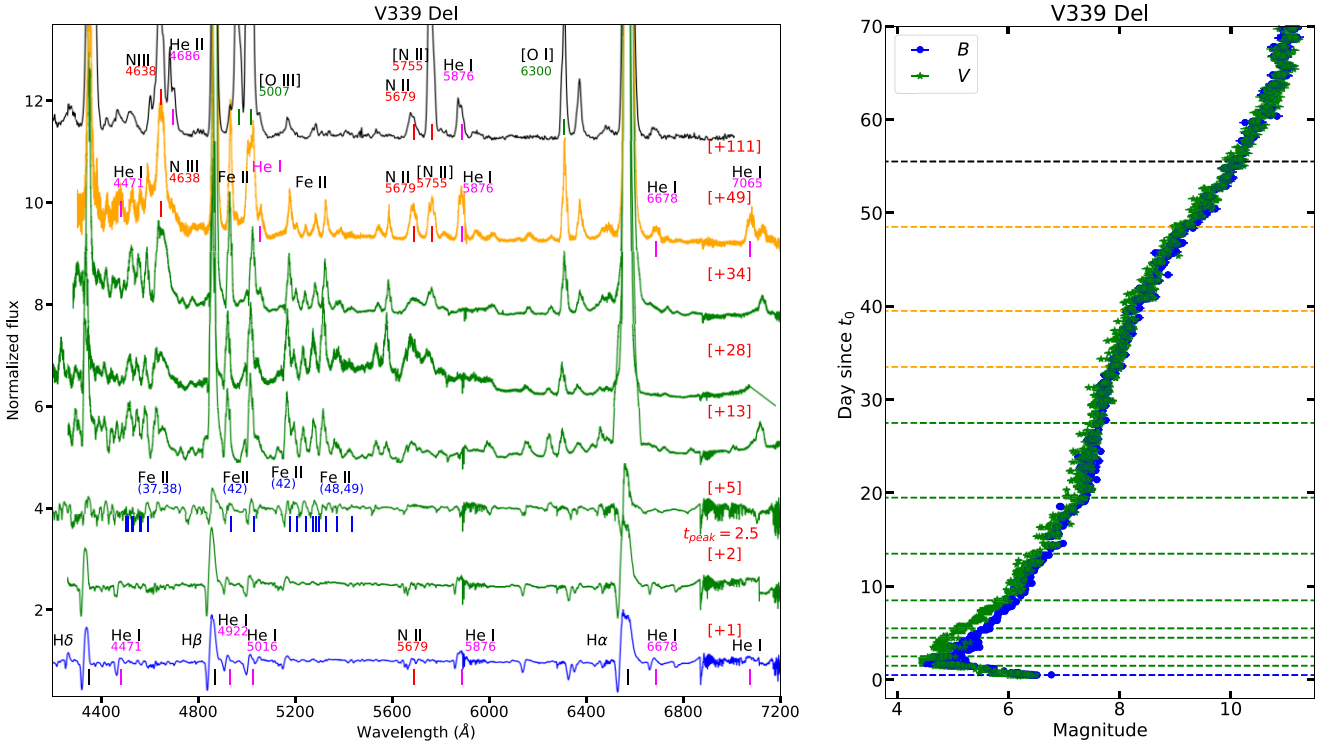

Figure 2. Same as Fig. 1 but for nova V339 Del.

duration) phase 1 (early He/N) or during a transition between phase 1 (early He/N) and phase 2 (Fe II). The Fe II lines dominated the spectrum until day 28 after t_0. After this, emission lines of He I, N III, and [N II] emerged and strengthened gradually until day around 50. Thereafter, strong emission lines of [O III], [O II], [N II], and He II emerged, indicating that the nova had entered the nebular phase. A detailed spectroscopic evolution of nova V339 Del is available in the supplementary online material.

Nova V659 Sct (ASASSN-19aad): The very fast Galactic nova V659 Sct was discovered by ASAS-SN on 2019 October 29.05 UT (HJD 2458785.55 $= t_0$), as ASASSN-19aad (Stanek & Kochanek 2019). The overall spectroscopic evolution of the nova and its optical light curve are presented in Fig. 3. The nova evolution was very fast, with $t_2 = 7$ d, while it reached optical peak in 2 d only since t_0. The first spectrum obtained for the nova, less than a day after discovery, showed P Cygni profiles of H Balmer, He I, and N III. A few days later, the He and N lines weakened, while emission lines of Fe II and Na I dominated the spectrum. By day 19, the spectrum is again dominated by a combination of He I, N III, [N II] emission lines, along with Fe ii and [O I]. The nova went into solar conjunction afterwards. spectroscopic observations taken over 200 d from t_0 showed strong forbidden lines of oxygen and nitrogen ([O III], [O II], and [N II]), implying that the nova has entered the nebular phase (Fig. 3).

Nova V1405 Cas: The very slow Galactic classical nova V1405 Cas was discovered by Yuji Nakamura on 2021 March 18.42 UT (HJD 2459291.92 $= t_0$). The overall spectroscopic evolution of the nova and its optical light curve are presented in Fig. 4. The nova took 53 d to reach the first visible peak. It also took more than 165 d (t_2) to decline by 2 mag from peak, as it stayed near visible peak for months, showing multiple flares (maxima). There are two major maxima/flares peaking on day $\approx$ 53 and day $\approx$ 130, at $V = 5.1$ and $V = 5.7$, respectively. The light curve also showed multiple smaller-amplitude flares peaking on days around 79, 92, 103, 175, 187, 205, and 2016. Between days 1 and 19 after t_0, the spectra of V1405 Cas were dominated by P Cygni profiles of Balmer and He II lines. From day 32 up to day around 100, the He I lines weakened significantly and Fe II P Cygni lines of the (42, 48, and 49) multiplets emerged and dominated the spectra (apart from the Balmer lines). Thereafter, the nova showed an oscillatory behaviour where at some epochs the Fe II lines were dominant, while in other epochs the He I lines were the dominant ones. This oscillatory behaviour is accompanied with the appearance of flares in the optical the light curve (Fig. 4). We further elaborate on this oscillatory behaviour in Section 4. After day 340, [O III] nebular lines emerge, implying that the nova has approached the nebular phase.

Nova V606 Vul: the slow Galactic classical nova V606 Vul was discovered by Koichi Itagaki on 2021 July 16.47 UT (HJD 2459411.97). Pre-discovery observations by the Zwicky Transient Facility (ZTF; Masci et al. 2019) show that the eruption started by 2021 June 15.38 UT (HJD 2459410.88 $= t_0$; Sokolovsky et al. in preparation). The overall spectroscopic evolution of the nova and its optical light curve are presented in Fig. 5. The nova evolution was slow, with $t_2 = 87$ d, while it climbed to optical peak in 16 d. The optical light curve is characterized by two main flares (maxima), peaking on days around 16 and 63 (at $V \approx 10$), with several other smaller-amplitude flares across the first 4 months of the eruption. Similar to the spectral evolution of the other novae in our main sample, V606 Vul showed initially spectra dominated by P Cygni profiles of Balmer, He I, N II, and N III during the early rise to peak between days 1 and 3. Afterwards, the He and N lines faded while Fe II lines of the 42, 48, and 49 multiplets emerged (see Fig. 5). This phase lasted between days 5 and 113, before the Fe II lines weakened and high-excitation lines of He and N (permitted and forbidden) strengthened in the following epochs (days 117 and 119). This was followed by a period of solar conjunction where the system was not observable. After V606 Vul emerged from solar conjunction, strong

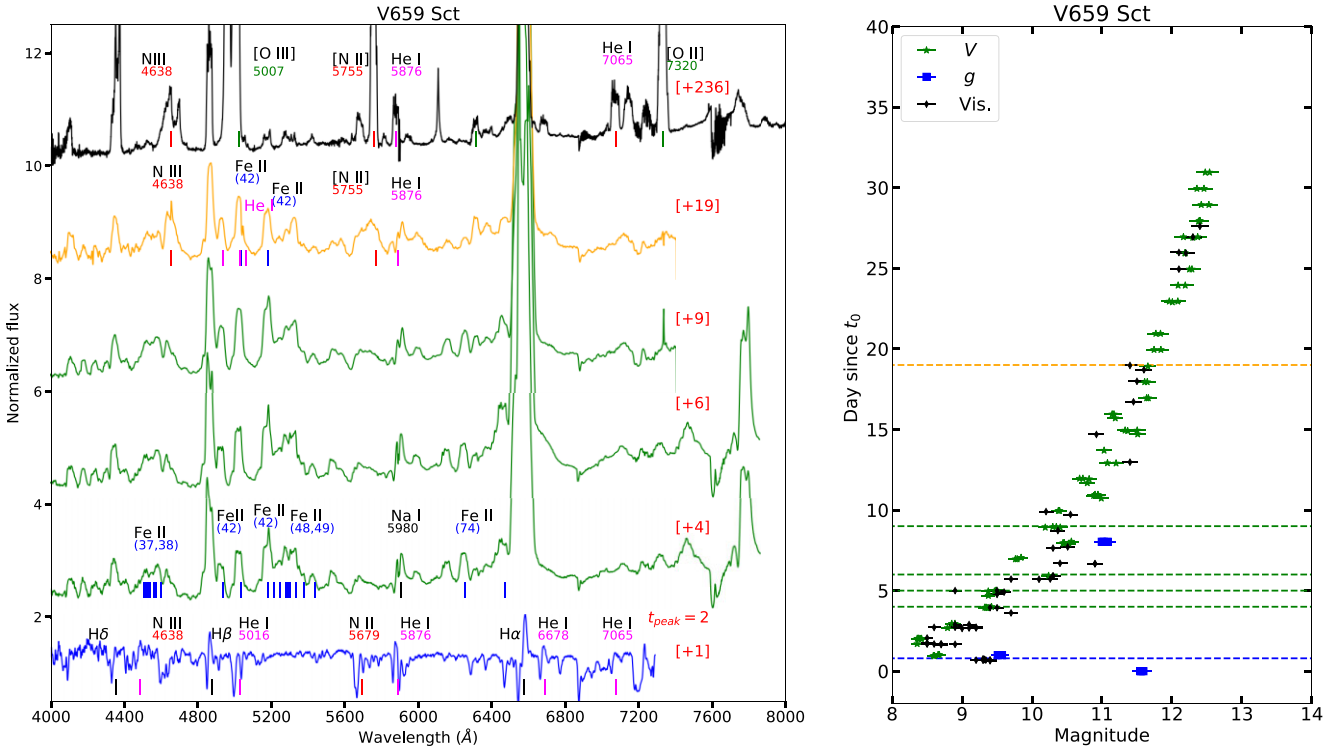

Figure 3. Same as Fig. 1 but for nova V659 Sct.

emission lines of forbidden, single and double ionized oxygen and nitrogen were in the spectrum, meaning that the nova already entered the nebular phase. A detailed spectroscopic evolution of nova V606 Vul is available in the supplementary online material.

*Gaia*22alz: The very slow Galactic nova *Gaia*22alz was reported on 2022 February 04.25 UT by *Gaia* alerts as an optical Galactic transient (Hodgkin et al. 2022). Pre-discovery photometry from ASAS-SN showed that the eruption started as early as 2022 January 25.02 UT (HJD 2459604.52 $= t_0$; see Aydi et al. 2023 for more details). The overall spectroscopic evolution of nova *Gaia*22alz and its optical light curve are presented in Fig. 6. The nova evolution was very slow, with $t_2 = 207$ d. It also took 178 d for the nova to reach optical peak from t_0, making it the slowest rising nova in our sample. The first few epochs of this nova were dominated by emission lines and later P Cygni profiles, of Balmer, He I, N II, and N III between days 45 and 97. A detailed description of the early spectroscopic evolution of this nova is presented in Aydi et al. (2023). The He and N lines weakened and the Fe II lines of multiplets (42, 48, and 49) strengthened, as the nova climbed to optical peak between days 103 and 278. From day 310 onwards, the Fe II lines became less prominent, while He I, He II, [N II], N III emerged and dominated the spectra (in addition to Balmer lines). By day 497, we observe relatively strong [O III] line at 5007 Å, implying that the nova has approached the nebular phase. A detailed spectroscopic evolution of nova *Gaia*22alz is available in the supplementary online material.

3.2 Slow novae (traditionally Fe II)

In this section we present the early spectroscopic evolution of two novae (a slow and very slow one), which are traditionally classified as Fe ii class. These novae show comparable behaviour to the novae above, but lack coverage for all four phases. We focus on their early spectroscopic evolution, demonstrating that they show evidence for early He/N spectral features (phase 1), if caught early enough. Further we describe these two slow novae:

V612 Sct (ASASSN-17hx): The very slow Galactic nova V612 Sct was discovered by ASAS-SN on 2017 June 19.41 as ASASSN-17hx (see Stanek et al. 2017 and Stanek & ASAS-SN Team 2017). The nova was monitored extensively by the ARAS group, and it showed Balmer and He I lines before developing strong Fe II features. The early spectroscopic evolution of the nova and its optical light curve are presented in Fig. 7. The nova rose to peak in 40 d. A long gap in the spectroscopic monitoring of the nova due to solar conjunction prevents us from building a complete spectral evolution. It also prevents us from constraining t_2, which we estimate it to be longer than 172 d, implying that V612 Sct is a very slow evolving nova. Nevertheless, the early spectra (days 6 and 10) show that the nova exhibits an early He/N phase before the Fe II P Cygni profiles dominated the spectra (after day 11). FM Cir: The slow Galactic nova FM Cir was discovered by John Seach on 2018 January 19.7 and classified as an Fe II nova by Strader et al. 2018. Pre-discovery observations from ASAS-SN show that the eruption started before or by 2018 January 17.87. The early spectroscopic evolution of the nova and its optical light curve are presented in Fig. 8. The nova evolution was very slow, with $t_2 = 120$ d, while it took 25 d since t_0 to reach optical peak. The first spectroscopic epoch taken on day 3 shows a combination of Balmer and both FeII and He/N P Cygni lines, implying that the nova was first observed during a transition phase between phase 1 and phase 2. Thereafter, the spectra are dominated by Balmer and Fe II P Cygni lines. We only focus on the early spectral evolution during the first two weeks of nova FM Cir to highlight that traditionally classified FeII slow novae also show an early He/N phase, emphasizing that the universal spectral evolution proposed in this work is ubiquitous. We lack further follow up to show the complete spectral evolution of this slow nova.

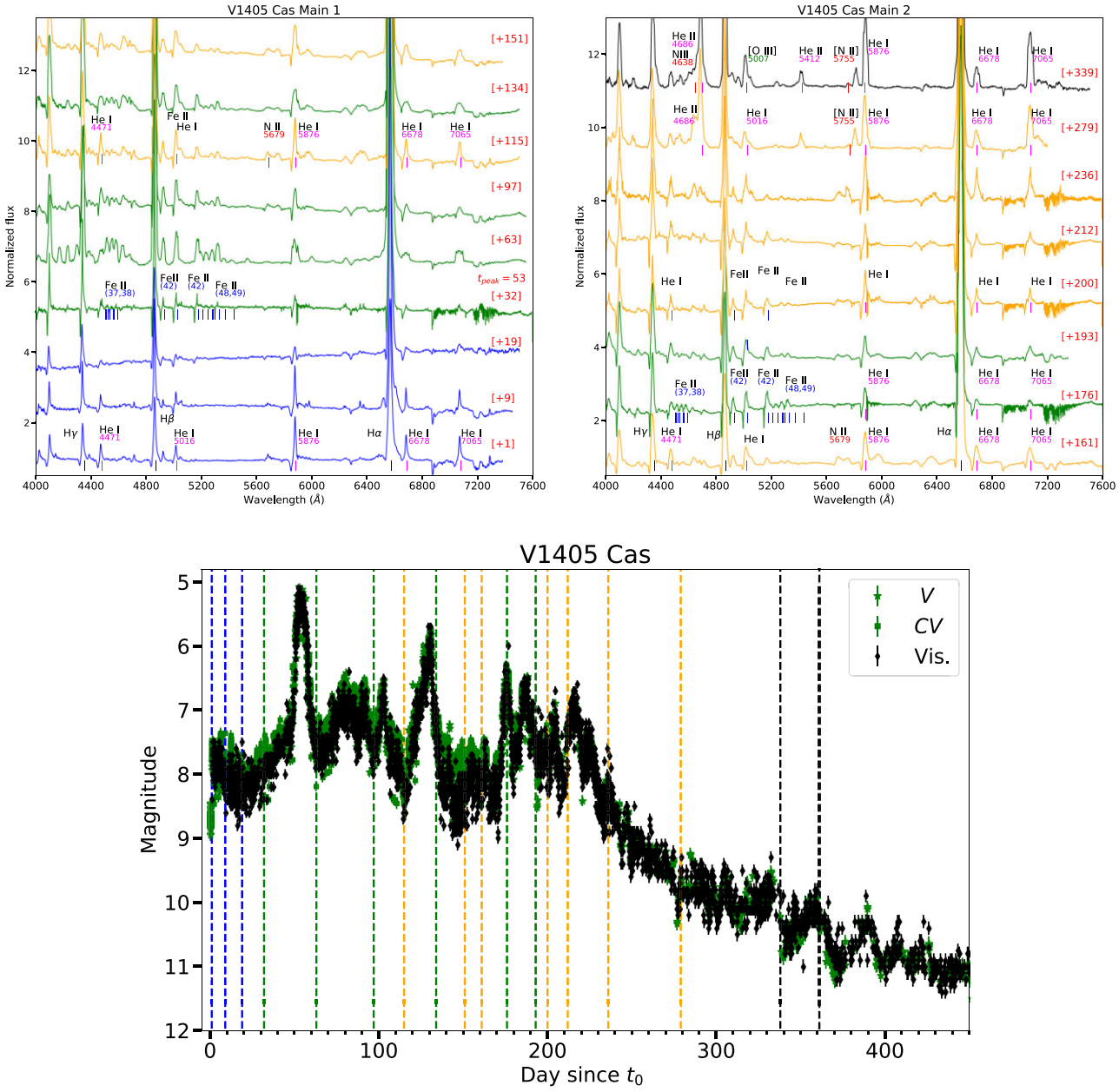

Figure 4. Same as Fig. 1 but for nova V1405 Cas.

3.3 The very fast novae (traditionally He/N)

In this section we present the early (first few days) spectral evolution of two very fast novae, which are traditionally classified as He/N novae. We show that even very fast novae exhibit a similar spectral evolution to the one described in our main sample. However, the main difference lies in the duration of phases 1 and 2, which tend to be very rapid (a few hours to a couple of days) and thus are easily missed. Nevertheless, dedicated follow up for these two very fast novae during the early hours/days of the eruption provide us with an opportunity to showcase their early spectral evolution. Further we describe the two fast novae:

V407 Lup: The very fast nova V407 Lup was discovered by ASAS-SN as ASASSN-16kt on 2016 September 24.00 (HJD 2457655.5 = t_0; Stanek & Team 2016; Stanek et al. 2016). The nova is characterized by t_2 <3 d (Aydi et al. 2018), implying that it is one of the fastest novae in the past decade. The nova rose to optical peak from the time of discovery in 1.4 d, highlighting its rapid evolution. The spectroscopic evolution of the nova over the first three weeks of eruption and its optical light curve are presented in Fig. 9. The first spectroscopic epoch, obtained less than a day after discovery, shows P Cygni lines of Balmer and He I. The second epoch was already 5 d later, showing significant differences in comparison to the earlier epoch. The spectrum is now dominated by broad emission lines of Balmer, He I, and N III, with some weak Fe II emission lines, at 4924, 5018, and 5169 Å (multiplet 42) and at 5317 Å (multiplet 48). The lines at 4924 and 5018 Å are likely blended and dominated by nearby He I lines at 4922 and 5016 Å (see Fig. A1). Given the line blending in this particular region, it is challenging to confirm the identity of all the lines in the spectra. The Fe II lines at 5169 and 5317 Å could conceivably be N II lines 5176 Å (multiplet 70) and 5320 Å (multiplet 69), which has been suggested to be present in the

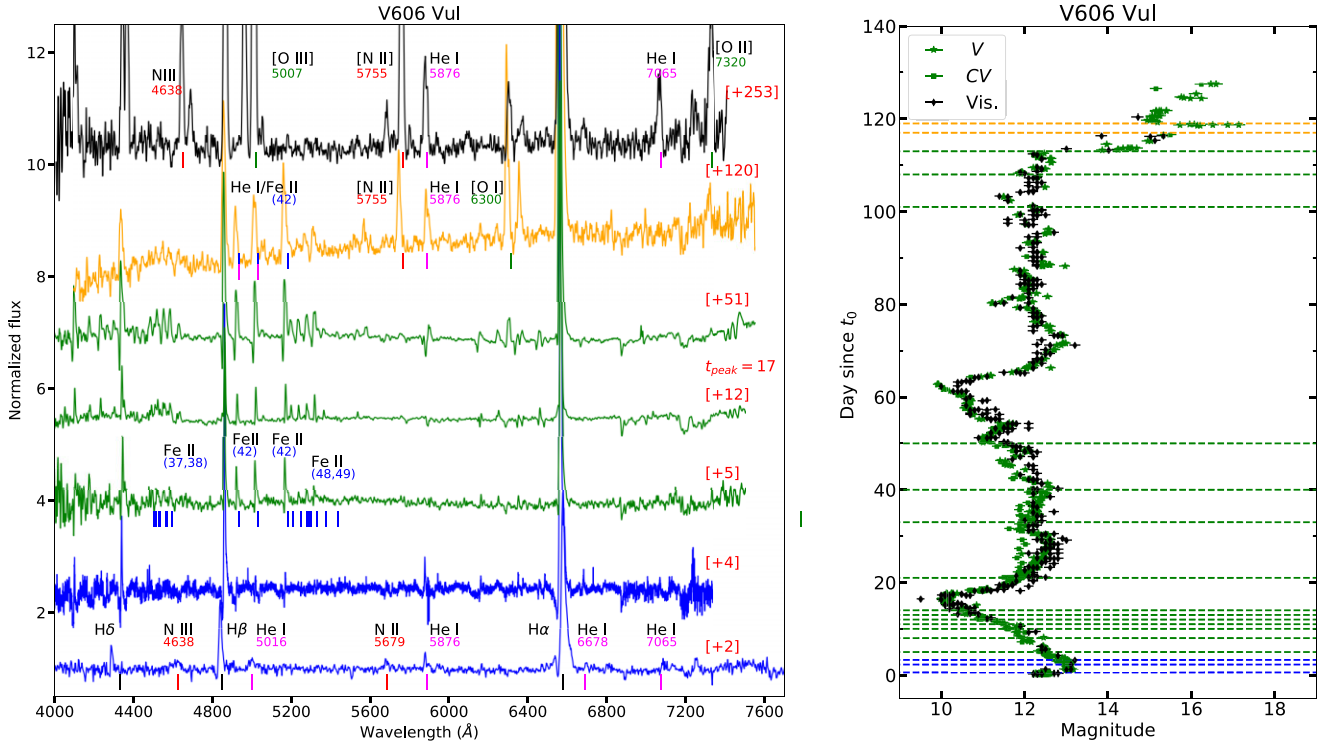

Figure 5. Same as Fig. 1 but for nova V606 Vul.

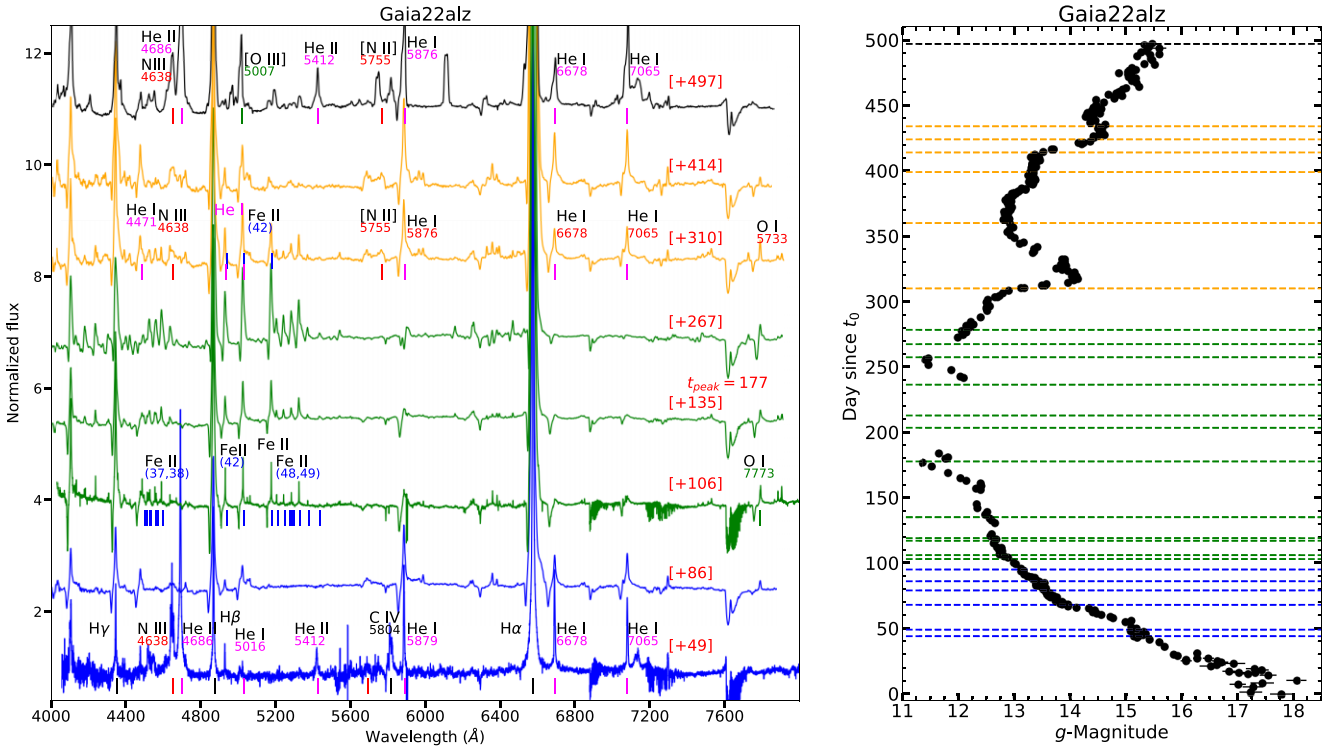

Figure 6. Same as Fig. 1 but for nova *Gaia*22alz.

spectra of some other novae (e.g. Munari et al. 2006). However, N II 5320 Å (69) is a quintet transition where the upper level is an auto-ionization state with a large excitation potential ≈ 30 eV (Bashkin & Stoner 1975). Because N III has a doublet $2p\,^2P^o$ ground state, a quintet multiplet like N II (69) cannot be directly populated by either electron recombination with N III or by resonance scattering of N II with its $2p^2\,^3P$ ground state. If N II 5320 Å of the (69) multiplet were to be present, another line of the same multiplet should be present at 5351 Å with similar intensity (Moore 1945), which is not the case as shown in Fig. A1. Moreover, the Fe II lines multiplet (42) and (48) are

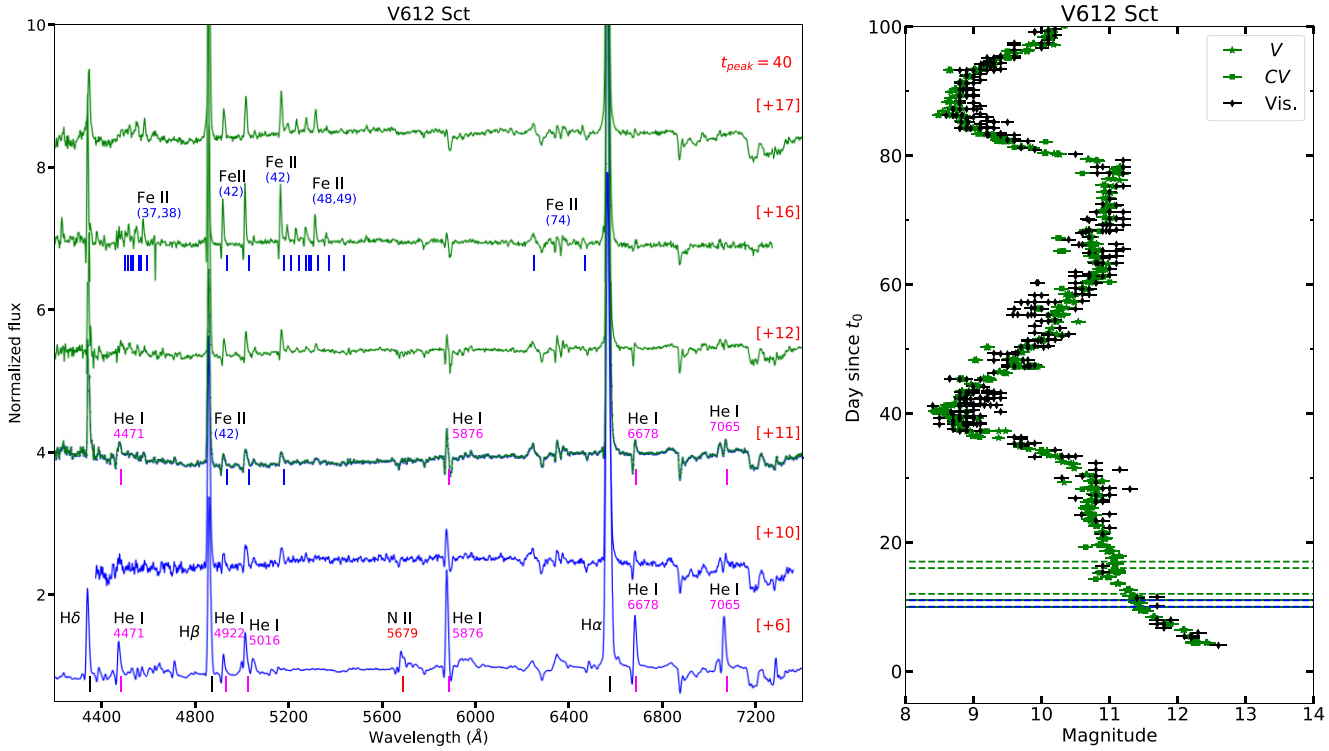

Figure 7. Same as Fig. 1 but for nova V612 Sct. The spectrum on day 11 is plotted in both green and blue, indicating that this epoch is a transition from phase 1 to phase 2.

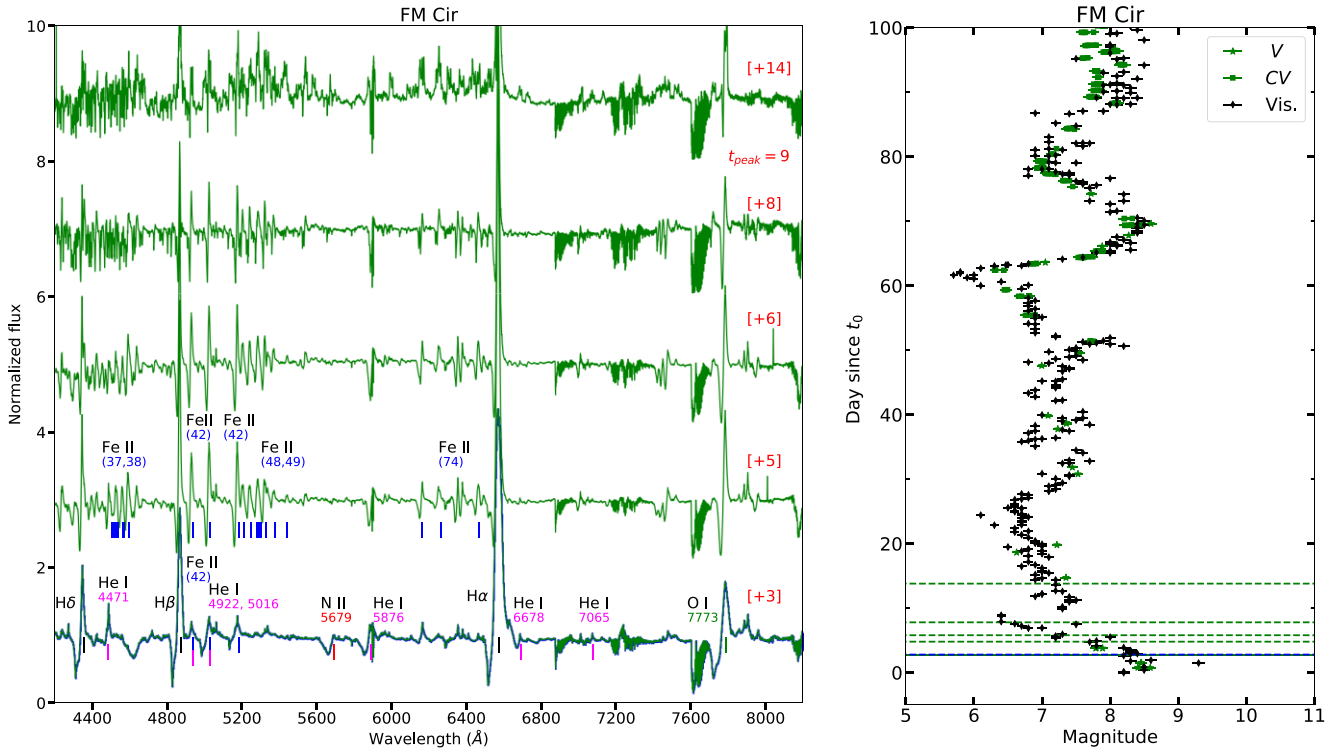

Figure 8. Same as Fig. 1 but for nova FM Cir. The spectrum on day 3 is plotted in both green and blue, indicating that this epoch is a transition from phase 1 to phase 2.

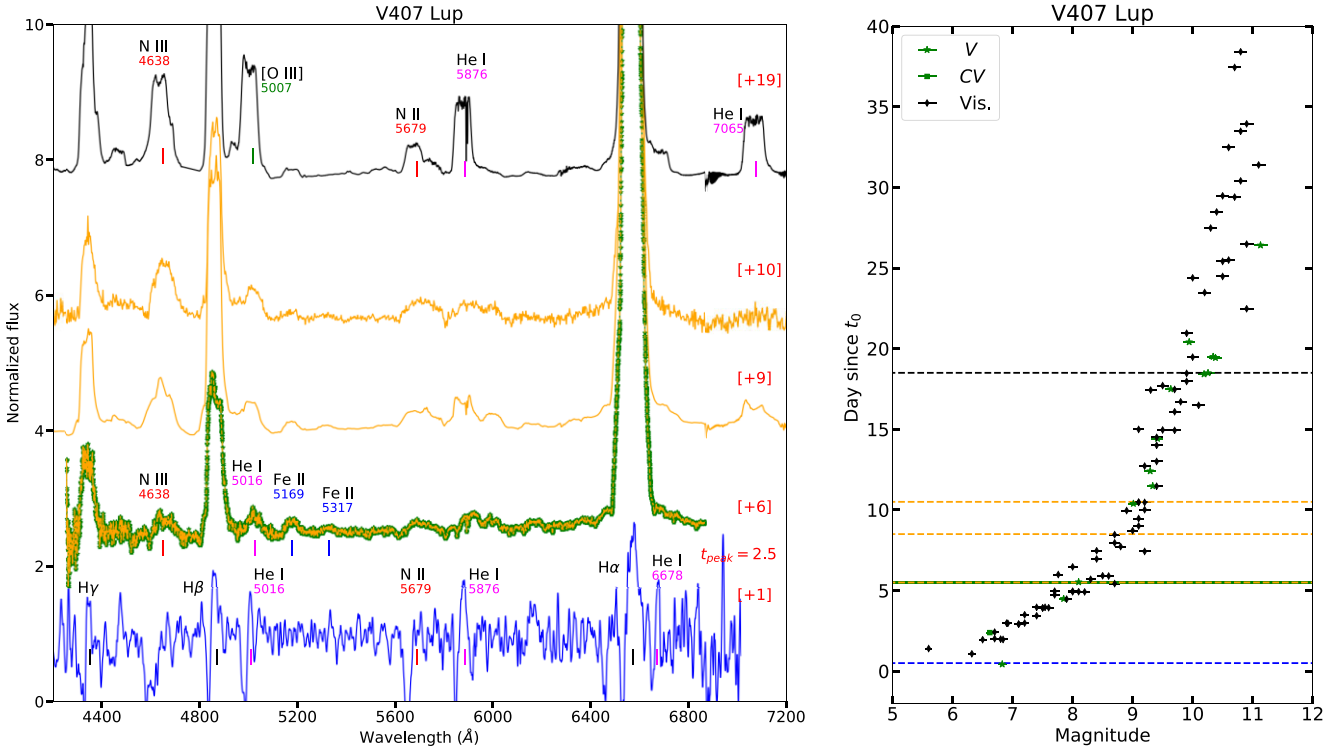

Figure 9. Same as Fig. 1 but for nova V407 Lup. The spectrum on day 6 is plotted in both green and red, indicating that this epoch is a transition from phase 2 to phase 3.

more common in nova spectra and are easier to form, compared to the N II lines multiplet (69) and (70). All this makes the identification of these lines as Fe II (42) and (48), rather than N II (69) and (70), more likely.

Due to the presence of these weak Fe II emission lines in the spectra of V407 Lup, Izzo et al. (2018) suggested that the nova had a very rapid iron curtain phase (see subsection 4.1). We also suggest that indeed, during this epoch the nova was captured in a transition phase between a rapid phase 2 and phase 3. It is possible that if the nova was observed between day 1 and day 6, we might have detected stronger Fe II lines, however, no observations are available during this phase. The He/N emission lines remained strong until day 10. By day 19, strong forbidden lines of O and N emerged, indicating that the nova has approached/entered the nebular phase. The spectroscopic evolution of nova V407 Lup again shows, that very fast novae, which are traditionally classified as He/N novae, also goes through the 3 main phases proposed in this work, while the first 2 phases (early He/N and Fe II) are very rapid compared to other novae. Moreover, phase 2 here is not as pronounced as for the novae in our main sample, since only a few Fe II lines emission lines are marginally detected.

U Sco (2022): The 2022 eruption of the recurrent Galactic nova U Sco was discovered on 2022 June 06.72 (HJD 2459737.22 $= t_0$) by Masayuki Moriyama. The eruption is characterized by a very rapid decline with $t_2 \approx 2 \pm 0.5$ d. It also rose to visible peak from t_0 in just half a day. The early spectroscopic evolution of the nova and its optical light curve are presented in Fig. 10. Nova U Sco shows extremely rapid changes in the spectra during the early days of the eruption, however, due to unprecedented dedicated follow up by both professional and citizen scientists, it was possible to disentangle the spectroscopic evolution of the nova during the first 2 d of the eruption with an immaculate cadence. The first spectroscopic epoch, taken 0.3 d after discovery, showed P Cygni lines of Balmer, He I, and N III. By day 0.7, the emission lines strengthened relative to the absorptions, and relatively weak Fe II lines of the (42) multiplet emerged. This possibly indicates that the nova went through an extremely rapid iron curtain phase, similar to the case of nova V407 Lup (likely even faster). The identification of the Fe II lines is also challenging due to the weakness of these lines and to blending with neighbouring lines. In Fig. A.2 we present zoom-in spectral plots focusing on the region of the Fe II (42), (48), and (55) multiplets. The plots show that some Fe II lines of these multiplets are possibly present in the spectra, but are weak relative to other lines of He I and Balmer. Some of them are also possibly blended with nearby stronger He I lines. While some of these lines could be N II 5176 Å and 5318 Å of the (70) and (69) multiplets as discussed for nova V407 Lup, the identification of these lines as Fe II (42 and 48 multiplets) is more reasonable, given the arguments presented in the previous section. By day 1.1, the absorption features almost disappear and the spectrum is dominated by broad emission lines of Balmer, He I, N II, and N III. This is an extreme case where spectral phases 1 and 2 lasted less than a day. Similar to V407 Lup, phase 2 here is not very pronounced, given the marginal detection of Fe II lines of the (42) and possibly (48) multiplet. However, the potential identification of some lines as Fe II, argue that very fast novae, like U Sco and V407 Lup go through a very rapid Fe II phase near peak, as they transition from phase 1 to phase 3.

4 DISCUSSION

4.1 A universal spectral evolution

The spectral evolution, traditionally dubbed 'hybrid' (where novae show a transition(s) between He/N and Fe II spectral features or show both He/N and Fe II features simultaneously Williams 2012), has been

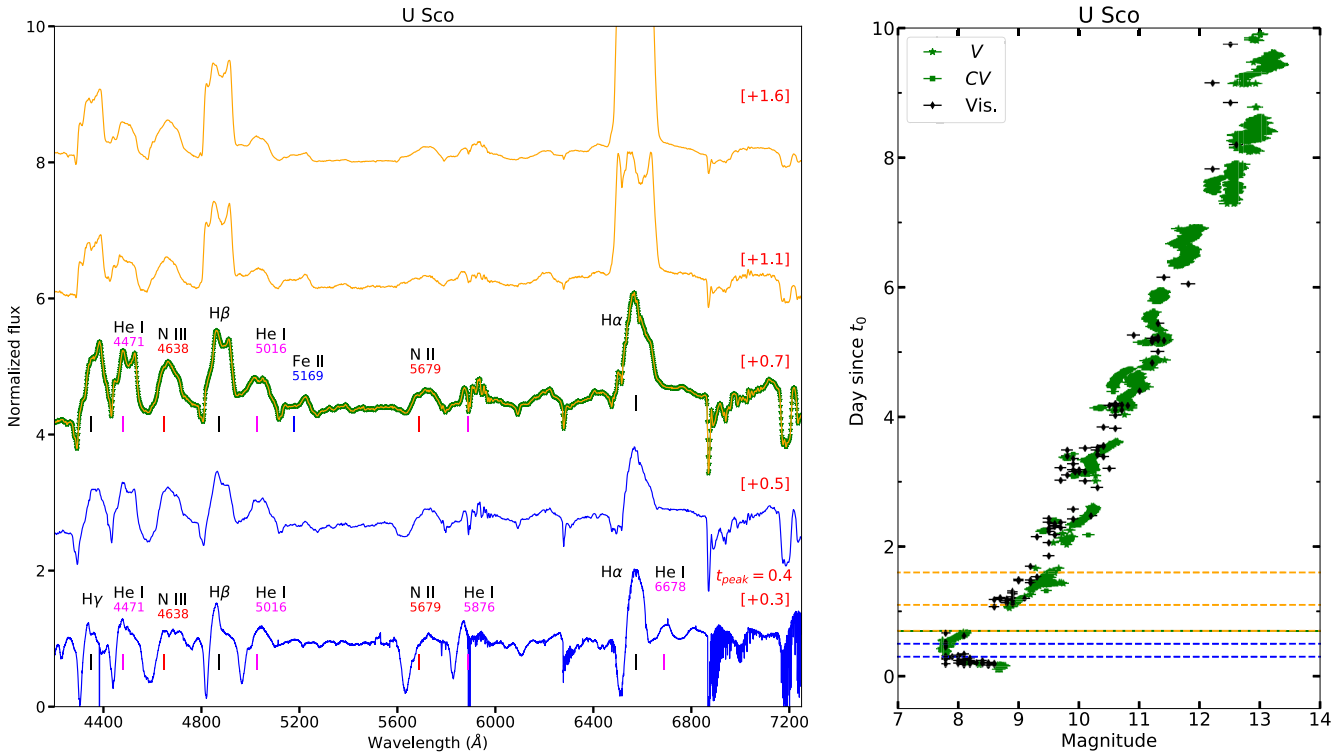

Figure 10. Same as Fig. 1 but for nova U Sco. The spectrum on day 0.7 is plotted in both green and red, indicating that this epoch is a transition from phase 2 to phase 3.

reported in the literature for several nova (e.g. V5558 Sgr; Tanaka et al. 2011b and T Pyx; Shore et al. 2011; Ederoclite 2014; Surina et al. 2014; Arai et al. 2015), and has been discussed theoretically (e.g. Shore 2012, 2014; Mason et al. 2018; Hachisu & Kato 2022). While the sample was still small, Williams (2012) suggested that all novae might be hybrid, but this needed to be confirmed by observations. Shore (2012, 2014) suggested that these classes are stages in the evolution of the nova and as the opacity and ionization of the ejecta changes throughout the eruption, the line dominating the spectra change. Therefore, the spectra naturally evolve from one class to another as the ejecta conditions change. Our results presented above are in agreement with these previous suggestions, and indicate that the spectral classes of He/N and Fe II are phases in the evolution of a nova and that the 'hybrid' (early He/N $\longrightarrow$ Fe II $\longrightarrow$ late He/N) evolution is likely universal in novae, regardless of their speed class. Further we offer a brief descriptive interpretation of the observations and the respective spectroscopic phases:

(i) Phase 1 (early He/N): this is an early phase of the eruption during the early rise to optical peak, at a stage where the nova ejecta are still hot (A few times 10^4 K; Hauschildt 2008) and dense (of the order of 10^{10} cm^{-3}; Metzger et al. 2016). That is, the presence of high-excitation lines of He I, N II, and N III, with P Cygni profiles implies that the nova ejecta are optically thick and relatively hot, with photospheric temperature of the order of a few times 10^4 K (Hauschildt 2008; Hachisu & Kato 2022). The high density is mostly due to the fact that the ejecta have not yet had enough time to expand. This early phase is relatively fast, lasting for only a few hours (e.g. nova U Sco) up to a few days (e.g. novae *Gaia*22alz and T Pyx). Therefore, it is often missed for most novae.

(ii) Phase 2 (Fe II): this phase manifests during the late rise to peak, at optical peak, and during the early decline. As the nova ejecta expand, they cool down rapidly, with the photospheric temperature reaching $\approx$ 8000 K around optical peak (Hauschildt 2008; Hachisu & Kato 2022). The expansion of the ejecta induces a recombination wave, leading to the emergence of P Cygni lines from neutral and lightly ionized heavy elements (such as Fe II, O I, and Na I). During this stage of the eruption, strong ultraviolet bands at 1500 – 1800 Å and 2300 – 2600 Å are reprocessed into less opaque, lower energies leading to the emergence of the Fe II lines in the optical – in the literature, it is often called the *iron curtain stage*. This phase, induced by expansion and cooling, lasts while the ejecta density is still high enough (a few times 10^{10} cm^{-3}; Shore 2008) to produce the low-ionization Fe II lines, before the density is too reduced by the continuing expansion (for a more detailed review, see Shore 2008, 2012, 2014). Therefore, for very fast novae with rapidly expanding ejecta, this Fe ii phase lasts for a short period (hours to a couple of days), such as the case of novae V407 Lup and U Sco. In this case the rapidly expanding ejecta might be photoionized to near nebular conditions in short period of time (hours/a few days), meaning that the *iron curtain stage* might not take place or take place for a very short time, so lines could appear at the same epoch from different regions in the ejecta, characterized by different densities (Shore 2008). This could explain the marginal detection of weak Fe II lines in the early spectra of U Sco and V407 Lup. However, for very slow novae with slowly expanding ejecta, the Fe II phase lasts for weeks and even months (e.g. V1405 Cas, FM Cir, and V612 Sct). Quoting from Shore (2008), '*we can say that virtually all novae pass through some Fe II-like stage*'.

(iii) Phase 3 (late He/N): this phase typically manifests during the late decline (2 – 5 magnitudes below optical peak). As the nova ejecta expand further and the mass-loss rate decreases, the ejecta drop in density and the photosphere recedes backwards to inner hotter regions due to the decrease in the optical depth ($\propto t^{-2}$). This leads to an increase in the ionization of the ejecta and eventually the *lifting of the iron curtain*. In the optical, this manifests as the

emergence of emission lines of high-excitation transitions such He I, He II, N II, N III, and [N II] (Hachisu & Kato 2022). Unlike, phase 1 where similar lines show P Cygni profiles, at this stage the lines show mostly emissions as the P Cygni absorptions become shallower.

The continuously expanding ejecta drop in density even further to a stage where the entire ejecta eventually become transparent and completely ionized, leading to the emergence of auroral and nebular lines particularly single and double ionized forbidden lines of oxygen, nitrogen, and eventually iron (Shore 2008). This so-called nebular phase succeeds phase 3 in most novae. Nevertheless, Williams (1992) showed that some novae do not develop strong nebular lines. This is mostly determined by the ejecta conditions (temperature and density) late in the eruption, e.g. if the supersoft emission (Wolf et al. 2013) turns off before the ejecta drop enough in density, it is possible that a nebular phase does not develop in the spectra (Cunningham, Wolf & Bildsten 2015).

We suggest that most if not all novae go through the three phases listed earlier, and that the Fe II and He/N spectroscopic classes are rather evolutionary phases during the eruption. That is, novae which are traditionally classified as Fe II novae are those that are caught during phase 2 near/after optical peak. Meanwhile, novae which are traditionally classified as He/N type are caught in phase 3 near/after peak, and represent systems wherein the first two phases are very rapid (lasting for $\sim$ hours), and are therefore missed. Novae that show features from both classes simultaneously are likely going through a transition between the phases (e.g. spectra of days 7 and 48 for T Pyx in Fig. 1, day 3 spectrum of FM Cir in Fig. 8, and day 6 spectrum of V407 Lup in Fig. 9). The line-driving presumably works primarily on the ion species that are prominent in the observed spectra at the time (Fe in the Fe II phase, He and N during the He/N phase), with other ion species being carried along passively via Coulomb friction. Whether the conditions are right for this to create regions of different abundances (see, e.g. Hunger & Groote 1999) should perhaps be investigated in the future.

One might argue that the (He/N $\longrightarrow$ Fe II$\longrightarrow$ He/N) evolution is only common in slowly evolving novae. However, since our sample consists of fast and slow novae, and since we see evidence for rapid phases 1 and 2 in very fast novae like U Sco, V407 Lup, and V659 Sct, our data indicate that the (He/N $\longrightarrow$ Fe II$\longrightarrow$ He/N) evolution is likely universal.

4.2 Origin in different bodies of gas?

Williams (2012) suggested that He/N spectra are consistent with an origin in the WD ejecta, whereas Fe II spectra point to formation in a large circumbinary envelope of gas whose origin is the secondary star. If this is the case, we should observe a large gradient in velocities between the Fe II lines in comparison to the He/N and Balmer lines, for the same nova – since the nova ejecta will be characterized by larger velocities (a few thousands km s^{-1}) compared to circumbinary-medium gas (dozens of km s^{-1}, e.g. as observed in symbiotic systems Mikołajewska 2012; Munari 2019). However, Aydi et al. (2020b) showed in their study of the early spectral evolution of novae and the dynamics of their ejecta that the Balmer lines, the Fe ii lines (particularly the prominent 42 multiplet), He lines, and the transient heavy elements absorption (THEA) lines all have similar velocities and show similar evolution. This led Aydi et al. (2020b) to conclude that the Fe lines and THEAs lines all originate in the nova ejecta, rather than originating in circumbinary material.

In Fig. 11 we show line profiles of Balmer, Fe II, and He I for nova *Gaia*22alz (one of the best monitored novae in our sample) on day

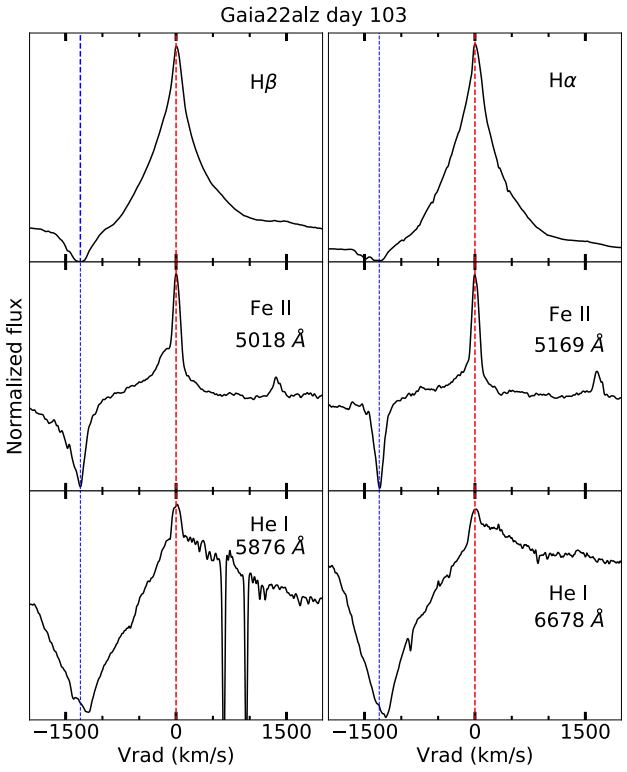

Figure 11. The profiles of Balmer (top), Fe II (middle), and He I (bottom) lines for nova *Gaia*22alz as observed 103 d after t_0. The red-dashed lines represent the peak wavelength of each line, while the green dashed lines represent $v = -1300$ km s^{-1} relative to the line peak.

103, at a stage of transition between phases 1 and 2, when both He and Fe features are present in the spectrum. The absorption troughs of the Balmer, Fe II, and He I P Cygni lines all have comparable blue-shifted velocities ranging between 1200 and 1300 km s^{-1}, implying that they originate in the same body of gas, that is, the nova ejecta. Nevertheless, the Fe II line structure is slightly different compared to the He I lines, which is not surprising since lines of different ionization potentials might originate at different depths/locations in the ejecta.

4.3 Interpretation in context of multiple ejections/outflows

Nova spectra are known to show multiple absorption and emission components at distinct velocities for the same species/lines, ranging between a few hundred up to a few thousand km s^{-1} (e.g. McLaughlin 1945; Payne-Gaposchkin 1957). There have long been suggestions that different line components are associated with different outflows or ejected shells (e.g. Friedjung 1966, 2011; Arai et al. 2016). More recently, Aydi et al. (2020b) suggested that all novae show evidence for at least two physically distinct outflows: an initial slow one manifesting as pre-maximum P Cygni profiles characterized by low velocities (a few hundred km s^{-1}), followed by a faster outflow which manifests as broader P Cygni components and emission lines with velocities of a few thousands km s^{-1}, emerging after maximum visible brightness. (Shen & Quataert 2022) suggested that the bulk (80–90 per cent) of the nova ejecta is carried by the slow flow, while the fast flow is less dense and carries a small fraction of the nova ejecta. So how does the spectral evolution suggested in this work fit with the multiple outflows scenario presented in previous studies such as McLaughlin (1945); Friedjung (1987, 2011); Arai et al. (2016);

Aydi et al. (2020b)? Do certain lines or ionization species originate in one of these outflows only?

The first He/N phase likely originates in the slow outflow during the early stages of its expansion. This early expansion of the slow flow manifests as P Cygni lines of Balmer and He/N, characterized by slow velocities (a few 100 km s^{-1}), which is the case for all the novae in our sample (see Figs 1–8). As the slow flow further expands, it cools down due to mainly adiabatic expansion, leading to a recombination phase, and the spectrum enters phase 2 (Fe II), developing P Cygni profiles of Balmer and Fe II (see, e.g. Fig. 1).

After peak, fast components emerge and are easily detected in some of the species/transitions. While the interpretation of Aydi et al. (2020b) was mostly based on the evolution of Balmer lines, where features from both outflows are easily visible, they also show that lines from heavier elements such as the Fe II (42) multiplet and some He I lines also show evidence for these two outflows. However, the less dense faster flow might not produce broad emission features in some of the transitions of heavy elements. For example, Aydi et al. (2020b) showed that the Fe II (42) multiplet lines develop fast components, while the (40) and (46) multiplet lines do not show such fast components. They suggest that the absence of fast components in these multiplets is due to their lower oscillator strength values, which might result in weak broad emission components from the low-density fast flow which are hardly detected. In slow novae, the ejecta is much denser compared to very fast novae, and therefore, even the fast flows have densities high enough to produce fast components in some of the Fe II lines, such as multiplet (42). However, in fast novae, the low-density fast flows might not develop any Fe II features.

As the outflows collide and merge, an intermediate velocity component emerge, which was named the principal component by McLaughlin (1945) and is suggested to become the dominant component in the spectra (Friedjung 1987). The velocity of the principal component is intermediate between the slow and fast components. The slow flow disappears shortly after peak, while the broad emission lines from the fast component become more difficult to resolve, as their intensity drops in comparison to the principal component which then dominates (see Aydi et al. 2020b). As the eruption evolves, lines of He I, N II, and, [N II] develop, characterized by velocities equivalent to that of the principal component. This evolution could either occur over weeks for slowly evolving novae or over hours/days for rapidly evolving novae.

As an example, we plot in Fig. 12 the line profiles of Hα, Fe II 5169 Å, and He I 6678 Å for nova V1405 Cas, one of our best observed novae. We select these lines because they are not blended with nearby lines. A few days before peak (during phase 2), we see P Cygni profiles with absorption troughs at velocities of around -700 km s^{-1}. During this phase, the He I lines are much weaker compared to the Fe II lines, but are still detectable. The 700 km s^{-1} reflects the velocity of the slow flow. After peak brightness, Hα shows a faster component reaching 2100 km s^{-1}. This velocity reflects the velocity of the fast flow. The Fe II and He I lines show velocities between 1000 and 1500 km s^{-1}, likely reflecting that of the intermediate (principal) component (Friedjung 1987). As the nova reaches phase 3, the Fe II lines disappear, while the He I emission lines show velocities of around 1200 km s^{-1}, again reflecting the velocity of the intermediate (principal) component.

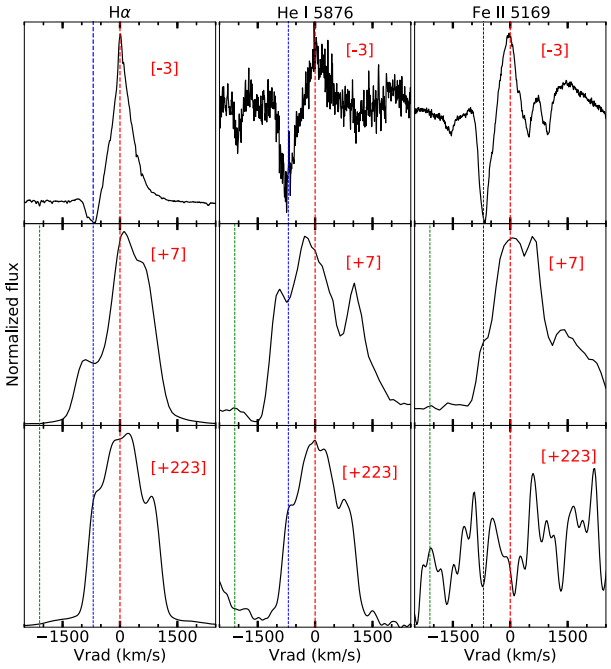

Figure 12. The profiles of Hα (left), He I (middle), and Fe II (right) lines for nova V1405 Cas. The numbers between brackets are days relative to visible peak brightness (day 56). The red-dashed lines represent the central wavelength of each line, while the blue and green-dashed lines represent $v = -700$ km s^{-1} and $v = -2100$ km s^{-1} relative to line center, respectively.

4.4 Interpretation in context of multiwavelength emission

Novae are panchromatic transients, emitting from radio to γ-rays (e.g. Chomiuk, Metzger & Shen 2021). As the nova ejecta expand, the peak of the spectral energy distribution shifts from optical to higher energies (first UV and then supersoft X-rays; Gallagher & Starrfield 1976, 1978; Page et al. 2013). More recently, the GeV γ-ray detection by the Large Area Telescope on board of the *Fermi* γ-ray satellite, highlighted the presence of strong energetic shocks (Ackermann et al. 2014; Cheung et al. 2016; Franckowiak et al. 2018), which might contribute a significant fraction of the nova visible luminosity (Metzger et al. 2015; Li et al. 2017; Aydi et al. 2020a). These shocks could also be the source of non-thermal hard X-ray (2 – 80 keV; Mukai & Ishida 2001; Mukai, Orio & Della Valle 2008; Sokolovsky et al. 2020; Aydi et al. 2020a; Gordon et al. 2021; Sokolovsky et al. 2022, 2023) and synchrotron radio emission (Finzell et al. 2018; Chomiuk, Metzger & Shen 2021). The shocks are suggested to occur at the interface of multiple phases of mass-loss, more particularly between an initial slow outflow, followed by a faster one (e.g. Chomiuk et al. 2014; Metzger et al. 2015; Aydi et al. 2020a, b). How does the optical spectral evolution presented in this work fit with the panchromatic emission in novae?

During the early rise to peak (early He/N phase), the ejecta are optically thick, and the emission from the remnant burning on the surface of the hot white dwarf is mostly absorbed by the dense ejecta, where it escapes in the visible. This is still true during the late rise to peak, when the spectra are cooling down, but still dense, exhibiting a shift into an Fe II spectra. Near peak, faster components emerge in different line species, coinciding with the detection of GeV γ-rays, originating from shock interaction (see previous section). Hard (2 – 80 keV) X-ray emission from the shocks are also detected (Sokolovsky et al. 2020, 2022), especially as the ejecta expand further and become more transparent (Gordon et al. 2021). Similarly, non-thermal synchrotron radio emission is observed at some stage during the eruption when the ejecta are transparent to the radio emission

(Chomiuk, Metzger & Shen 2021). This happens during the decline from peak, when the spectra are transitioning from the Fe II stage to the later He/N stage. As the ejecta expand even further (dropping more in density), the spectra start transitioning from the late He/N phase to the nebular phase, coinciding with the detection of supersoft X-ray emission in several novae (e.g. Page et al. 2013, 2015; Page, Beardmore & Osborne 2020). The beginning of the nebular phase usually marks the start of the supersoft emission phase. Around this stage, many novae also show a hike in the thermal radio flux, as the ejecta are now extended enough to produce strong thermal radio emission (Hjellming et al. 1979; Chomiuk, Metzger & Shen 2021).

4.5 An early phase preceding phase 1?

Arai et al. (2015) reported relatively narrow (FWHM $\approx 600\,\mathrm{km\,s^{-1}}$) emission lines of He II, N III, Balmer, and He I in the early spectra of T Pyx taken 0.2 d after the discovery of its 2012 eruption. These high-excitation lines of He II and N III disappear after a day, and the Balmer and He I lines develop P Cygni absorption components. Similarly, Aydi et al. (2023) recently reported high-excitation narrow (FWHM $\approx 300\,\mathrm{km\,s^{-1}}$) emission lines of N III, He II, and C IV in the early spectra of *Gaia*22alz, along with Balmer and He I lines. These high-excitation narrow emission lines also disappear as the nova evolves, and the Balmer and He I lines develop P Cygni profiles (see Fig. 6). The main difference between this early phase and phase 1 is the absence of P Cygni profiles, the presence of high-excitation lines, and the relatively slow velocities (FWHM of the lines if around 300–400 $\mathrm{km\,s^{-1}}$). Aydi et al. (2023) discussed different possible origins for these high-excitation narrow emission lines, and they concluded that they likely originate in a hot, optically thin nova envelope, which is not yet fully ejected and is reprocessing some of the high-energy emission from the white dwarf surface during the early UV/X-ray flash phase (e.g. Hillman et al. 2014; König et al. 2022).

It might be that this early and rarely observed phase precedes phase 1 in most novae, but it is extremely rapid and often missed. In the era of new all-sky surveys, we expect to detect more novae during their early rise, which would allow spectroscopic follow-up during these early and critical phases. Such early follow up could show spectra consistent with the early spectra of novae T Pyx and *Gaia*22alz, proving that this earlier phase, characterized by relatively narrow high-excitation emission lines, is common.

4.6 Oscillatory spectral behaviour in flaring novae

The spectroscopic evolution of the flaring nova V1405 Cas (Fig. 4) shows an oscillatory behaviour where the spectra oscillate between phases 2 and 3 multiple times, as the nova shows multiple maxima in its optical light curve (Fig. 4). During this stage, the spectra show both Fe II and He/N P Cygni lines, but the relative strength of these features vary. Such a behaviour has also been reported previously for other flaring novae (e.g. Tanaka et al. 2011a, b; Aydi et al. 2019). While determining the origin of the multiple flares/maxima in the optical light curves of novae is outside of the scope of this work, we briefly discuss potential explanations for the oscillatory spectral behaviour observed in such novae: (1) a change in the brightness of the central source leading to flares in the optical light curve and eventually a change in the radius of the photosphere. This change in the photosphere radius means that the emission could originate in different regions of the ejecta as a function of time (outer colder regions are dominated by low-ionization Fe II lines, while inner hotter regions lead to higher excitation lines of He I, He II, and N II); (2) multiple ejections, interacting with the previously existing ejecta and leading to flares in the optical light curves. These new ejections could lead to an increase in the density of the ejecta resulting in spectra dominated by Fe II lines. As the ejecta eventually expand, they drop in density leading to the emergence of He/N features. If the nova exhibits multiple ejections, we might observe multiple peaks in the light curve and an oscillatory behaviour in the spectra. Steinberg & Metzger (2020) discussed how multiple collisions between alternative fast/slow outflows can produce accelerating and decelerating line features and rapidly varying density structures.

5 CONCLUSIONS

In this work, we revisit pioneering studies from the past 2–3 decades (Williams 1992; Shore 2012; Williams 2012; Shore 2013, 2014), with the aim of discussing the origin of the Fe II and He/N spectroscopic classes of novae and testing some previous suggestions about the universality of certain spectral evolution where novae show features from both of these classes as a function of time since eruption (Shore 2008; Shore et al. 2011; Tanaka et al. 2011b; Ederoclite 2014; Surina et al. 2014). In order to do this, we present detailed spectral evolution of a sample of novae, throughout different phases of their eruptions (early rise, optical peak, early decline, and late decline), which is made possible by the era of new all-sky surveys and the collaboration between professional astronomers and citizen scientists Our data show that novae of different speed classes show a similar spectral evolution going through at least three spectral phases: phase 1 (early He/N) when the spectra are dominated by P Cygni lines of Balmer, He I, N II, and N III; phase 2 (Fe II), when the spectra are dominated by P Cygni lines of Balmer, Fe II, and O I; phase 3 (late He/N), when the spectra are dominated by emission lines of Balmer, He I, He II, N II, and N II. A fourth phase, dubbed the nebular phase, develops in many novae, when nebular forbidden lines of O I, O II, O III, and N II emerge and dominate the spectra. This evolution is primarily driven by changes in the opacity, ionization, temperature, and density of the nova ejecta, as previously suggested by Shore (2008, 2012, 2014).

Based on our data set, this evolution appears to be ubiquitous, whether the nova evolves rapidly or slowly, emphasizing that the traditional classes of Fe II and He/N are evolutionary phases that most if not all novae go through during their eruptions. The main difference is the duration of these phases, which could last for days/weeks for slow novae or hours/days for very fast novae. Traditionally classified Fe II novae are typically first caught in phase 2 near peak and they tend to be slow novae, where phase 2 lasts for days/weeks. While traditionally classified He/N novae are those typically first observed in phase 3 near peak and they tend to evolve rapidly, where phases 1 and 2 only last for a few hours/days, that is these early phases are easily missed. Therefore, cautious is required when assigning Fe II or He/N spectral classes to novae, as these classes are stages in the spectral evolution of a nova.

ACKNOWLEDGEMENTS

We thank the ARAS and AAVSO observers from around the world who contributed their spectra to the ARAS Data base and their magnitude measurements to the AAVSO International Data base, used in this work.

EA acknowledges support by NASA through the NASA Hubble Fellowship grant number HST-HF2-51501.001-A awarded by the Space Telescope Science Institute, which is operated by the Association of Universities for Research in Astronomy, Inc., for NASA,

under contract NAS5-26555. LC acknowledges NSF awards AST-1751874 and AST-2107070 and a Cottrell fellowship of the Research Corporation. JS was supported by the Packard Foundation. DAHB gratefully acknowledges the receipt of research grants from the National Research Foundation (NRF) of South Africa. AK acknowledges the Ministry of Science and Higher Education of the Russian Federation grant number 075-15-2022-262 (13.MNPMU.21.0003). BDM is supported in part by NASA (grants 80NSSC22K0807 and 80NSSC22K1573). JM was supported by the National Science Centre, Poland, grant OPUS 2017/27/B/ST9/01940. KJS is supported by NASA through the Astrophysics Theory Programme (80NSSC20K0544). AE acknowledge the financial support from the Spanish Ministry of Science and Innovation and the European Union – NextGenerationEU through the Recovery and Resilience Facility project ICTS-MRR-2021-03-CEFCA. A part of this work is based on observations made with the Southern African Large Telescope (SALT), with the Large Science Programme on transients 2021-2-LSP-001 (PI: DAHB). Polish participation in SALT is funded by grant number MEiN 2021/WK/01. This paper was partially based on observations obtained at the Southern Astrophysical Research (SOAR) telescope, which is a joint project of the Ministério da Ciência, Tecnologia e Inovações (MCTI/LNA) do Brasil, the US National Science Foundation's NOIRLab, the University of North Carolina at Chapel Hill (UNC), and Michigan State University (MSU). Analysis made significant use of PYTHON 3.7.4, and the associated packages NUMPY, MATPLOTLIB, SEABORN, SCIPY. Data reduction made significant use of MIDAS FEROS (Stahl, Kaufer & Tubbesing 1999), Echelle (Ballester 1992), PYSALT (Crawford et al. 2010), andIRAF (Tody 1986, 1993).

DATA AVAILABILITY

The data are available as online material and can be found here: https://www.dropbox.com/scl/fi/3kdnmu52lp8j6j2y7nclp/FeII_HeN_onine_data.zip?rlkey=u8gxya6q970cw18f46k804mqr&dl = 0. Supplementary plots can be found here: https://www.dropbox.com/scl/fi/0glj9qxgj6zoj884qox1k/FeII_HeN_online_plots.zip?rlkey=ml04qp2v2b6ylos5fn97zwvt6&dl = 0.

REFERENCES

Ackermann M. et al., 2014, Science, 345, 554
Arai A., Isogai M., Yamanaka M., Akitaya H., Uemura M., 2015, Acta Polytechnica CTU Proceedings, 2, 257
Arai A., Kawakita H., Shinnaka Y., Tajitsu A., 2016, ApJ, 830, L30
Aydi E. et al., 2018, MNRAS, 480, 572
Aydi E. et al., 2019, preprint (arXiv:1903.09232)
Aydi E., Chomiuk L., Sokolovsky K. V., Steinberg E., 2020a, Nat. Astron., 2, 697
Aydi E. et al., 2020b, ApJ, 905, L62
Aydi E. et al., 2023, MNRAS, 524, 1946
Ballester P., 1992, in Grosbøl P. J., de Ruijsscher R. C. E., eds, European Southern Observatory Conf. and Workshop Proc., Vol. 41. p. 177
Barnes S. I. et al., 2008, in McLean I. S., Casali M. M., eds, Proc. SPIE Conf. Ser. Vol. 7014, Ground-based and Airborne Instrumentation for Astronomy II. SPIE, Bellingham, p. 70140K
Bashkin S., Stoner J. O., 1975, Atomic energy levels and Grotrian Diagrams – Vol.1: Hydrogen I – Phosphorus XV; Vol.2: Sulfur I – Titanium XXII. North-Holland Publ. Co., Amsterdam
Bode M. F., Evans A., 2008, in Bode M. F., Evans A., eds, Cambridge Astrophys. Ser. No. 43, Classical Novae, 2nd edn. Cambridge Univ. Press, Cambridge
Bramall D. G. et al., 2010, in McLean I. S., Ramsay S. K., Takami H., eds, Proc. SPIE Conf. Ser. Vol. 7735, Ground-based and Airborne Instrumentation for Astronomy III. SPIE, Bellingham, p. 77354F
Bramall D. G. et al., 2012, in McLean I. S., Ramsay S. K., Takami H., eds, Proc. SPIE Conf. Ser. Vol. 8446, Ground-based and Airborne Instrumentation for Astronomy IV. SPIE, Bellingham, p. 84460A
Buckley D. A. H., Swart G. P., Meiring J. G., 2006, in McLean I. S., Casali M. M., eds, Proc. SPIE Conf. Ser. Vol. 6267, Commissioning of the Southern African Large Telescopes (SALT) first generation instruments. SPIE, Bellingham, p. 62670Z
Burgh E. B., Nordsieck K. H., Kobulnicky H. A., Williams T. B., O'Donoghue D., Smith M. P., Percival J. W., 2003, in Iye M., Moorwood A. F. M., eds, Proc. SPIE Conf. Ser. Vol. 4841, Instrument Design and Performance for Optical/Infrared Ground-based Telescopes. SPIE, Bellingham, p. 1463
Cheung C. C. et al., 2016, ApJ, 826, L142
Chomiuk L. et al., 2014, Nature, 514, 339
Chomiuk L., Metzger B. D., Shen K. J., 2021, ARA&A, 59, 391
Clemens J. C., Crain J. A., Anderson R., 2004, in Moorwood A. F. M., Iye M., eds, Proc. SPIE Conf. Ser. Vol. 5492, Ground-based Instrumentation for Astronomy. SPIE, Bellingham, p. 331
Crause L. A. et al., 2014, in Ramsay S. K., McLean I. S., Takami H., eds, Proc. SPIE Conf. Ser. Vol.9147, Ground-based and Airborne Instrumentation for Astronomy V. SPIE, Bellingham, p. 91476T
Crawford S. M. et al., 2010, in Silva D. R., Peck A. B., Soifer B. T., eds, Proc. SPIE, Conf. Ser. Vol. 7737, Observatory Operations: Strategies, Processes, and Systems III. SPIE, Bellingham, p. 773725
Cunningham T., Wolf W. M., Bildsten L., 2015, ApJ, 803, L76
Della Valle M., Izzo L., 2020, A&A Rev., 28, 3
Ederoclite A., 2014, in Woudt P. A., Ribeiro V. A. R. M., eds, ASP Conf. Ser. Vol. 490, Stellar Novae: Past and Future Decades. Astron. Soc. Pac., San Francisco, p. 163,
Finzell T. et al., 2018, ApJ, 852, L108
Franckowiak A., Jean P., Wood M., Cheung C. C., Buson S., 2018, A&A, 609, 120
Friedjung M., 1966, MNRAS, 131, 447
Friedjung M., 1987, A&A, 180, 155
Friedjung M., 2011, A&A, 536, A97
Gallagher J. S., Starrfield S., 1976, MNRAS, 176, 53
Gallagher J. S., Starrfield S., 1978, ARA&A, 16, 171
Gordon A. C., Aydi E., Page K. L., Li K.-L., Chomiuk L., Sokolovsky K. V., Mukai K., Seitz J., 2021, ApJ, 910, L134
Hachisu I., Kato M., 2022, ApJ, 939, L1
Hauschildt P. H., 2008, in Bode M. F., Evans E. A., eds, Cambridge Astrophys. Ser., No. 43, Classical Novae. Cambridge Univ. Press, Cambridge, p. 77
Hillman Y., Prialnik D., Kovetz A., Shara M. M., Neill J. D., 2014, MNRAS, 437, 1962
Hjellming R. M., Wade C. M., Vandenberg N. R., Newell R. T., 1979, AJ, 84, 1619
Hodgkin S. T. et al., 2022, Transient Name Server Discovery Report, 2022-313, 1
Hunger K., Groote D., 1999, A&A, 351, 554
Izzo L. et al., 2018, MNRAS, 478, 1601
Kaufer A., Stahl O., Tubbesing S., Nørregaard P., Avila G., Francois P., Pasquini L., Pizzella A., 1999, The Messenger, 95, 8
Kloppenborg B. K., 2023, Observations from the AAVSO International Data base, available at: https://www.aavso.org
Kniazev A. Y., Gvaramadze V. V., Berdnikov L. N., 2016, MNRAS, 459, 3068
Kniazev A. Y., Usenko I. A., Kovtyukh V. V., Berdnikov L. N., 2019, Astrophys. Bull., 74, 208
Kobulnicky H. A., Nordsieck K. H., Burgh E. B., Smith M. P., Percival J. W., Williams T. B., O'Donoghue D., 2003, in Iye M., Moorwood A. F. M., eds, Proc. SPIE Conf. Ser. Vol. 4841, Instrument Design and Performance for Optical/Infrared Ground-based Telescopes. SPIE, Bellingham, p. 1634
König O. et al., 2022, Nature, 605, 248
Li K.-L. et al., 2017, Nat. Astron., 1, 697
Masci F. J. et al., 2019, PASP, 131, 018003

Mason E., Shore S. N., De Gennaro Aquino I., Izzo L., Page K., Schwarz G. J., 2018, ApJ, 853, L27
McLaughlin D. B., 1944, Popular Astronomy, 52, 109
McLaughlin D. B., 1945, PASP, 57, 69
Mclaughlin D. B., 1947, PASP, 59, 244
Metzger B. D., Finzell T., Vurm I., Hascoët R., Beloborodov A. M., Chomiuk L., 2015, MNRAS, 450, 2739
Metzger B. D., Caprioli D., Vurm I., Beloborodov A. M., Bartos I., Vlasov A., 2016, MNRAS, 457, 1786
Mikołajewska J., 2012, Baltic Astron., 21, 5
Moore C. E., 1945, Contributions from the Princeton University Observatory, Vol. 20
Mukai K., Ishida M., 2001, ApJ, 551, L1024
Mukai K., Orio M., Della Valle M., 2008, ApJ, 677, L1248
Munari U., 2019, The Impact of Binary Stars on Stellar Evolution, 54, 77
Munari U., Siviero A., Navasardyan H., Dallaporta S., 2006, A&A, 452, 567
Nakano S. et al., 2013, Central Bureau Electronic Telegrams, 3628, 1
O'Donoghue D. et al., 2006, MNRAS, 372, 151
Page M. J. et al., 2013, MNRAS, 436, 1684
Page K. L. et al., 2015, MNRAS, 454, 3108
Page K. L., Beardmore A. P., Osborne J. P., 2020, Adv. Space Res., 66, 1169
Payne-Gaposchkin C. H. P., 1957, The Galactic Novae. Amsterdam, North-Holland Pub. Co., New York, Interscience Publishers
Schaefer B. E., 1990, ApJ, 355, L39
Schaefer B. E. et al., 2013, ApJ, 773, L55
Shappee B. J. et al., 2014, ApJ, 788, L48
Shen K. J., Quataert E., 2022, ApJ, 938, L31
Shore S. N., 2008, in Bode M. F., Evans E. A., eds, Cambridge Astrophys. Ser. No. 43, Classical Novae. Cambridge Univ. Press, Cambridge, p. 194
Shore S. N., 2012, Bull. Astron. Soc. India, 40, 185
Shore S. N., 2013, A&A, 559, 7
Shore S. N., 2014, in Woudt P. A., Ribeiro V. A. R. M., eds, ASP Conf. Ser. Vol. 490, Stellar Novae: Past and Future Decades. Astron. Soc. Pac., San Francisco, p. 145
Shore S. N., Augusteijn T., Ederoclite A., Uthas H., 2011, A&A, 533, 8
Sokolovsky K. V. et al., 2020, MNRAS, 497, 2569
Sokolovsky K. V. et al., 2022, MNRAS, 514, 2239
Sokolovsky K. V. et al., 2023, MNRAS, 521, 5453
Stahl O., Kaufer A., Tubbesing S., 1999, in Guenther E., Stecklum B., Klose S., eds, ASP Conf. Ser. Vol. 188, Optical and Infrared Spectroscopy of Circumstellar Matter. Astron. Soc. Pac., San Francisco, p. 331
Stanek K. Z., ASAS-SN Team, 2017, ATel, 10524, 1
Stanek K. Z., Kochanek C. S., 2019, Transient Name Server Discovery Report, 2019-2216, 1
Stanek K. Z., Team A.-S., 2016, ATel, 9539, 1
Stanek K. Z. et al., 2016, ATel, 9538, 1
Stanek K. Z. et al., 2017, ATel, 10523, 1
Steinberg E., Metzger B. D., 2020, MNRAS, 491, 4232
Strader J., Chomiuk L., Swihart S., Shishkovsky L., 2018, ATel, 11209, 1
Surina F., Hounsell R. A., Bode M. F., Darnley M. J., Harman D. J., Walter F. M., 2014, AJ, 147, 107
Tanaka J., Nogami D., Fujii M., Ayani K., Kato T., 2011a, PASJ, 63, 159
Tanaka J., Nogami D., Fujii M., Ayani K., Kato T., Maehara H., Kiyota S., Nakajima K., 2011b, PASJ, 63, 911
Teyssier F., 2019, Contrib. Astron. Obs. Skaln. Pleso, 49, 217
Tody D., 1986, in Crawford D. L., ed., Proc. SPIE Conf. Ser. Vol. 627, Instrumentation in Astronomy VI. SPIE, Bellingham, p. 733
Tody D., 1993, in Hanisch R. J., Brissenden R. J. V., Barnes J., eds, ASP Conf. Ser. Vol. 52, Astronomical Data Analysis Software and Systems II. Astron. Soc. Pac., San Francisco, p. 173
Williams R. E., 1992, AJ, 104, 725
Williams R. E., 2012, AJ, 144, 98
Williams R., Mason E., Della Valle M., Ederoclite A., 2008, ApJ, 685, L451
Wolf W. M., Bildsten L., Brooks J., Paxton B., 2013, ApJ, 777, L136
Wren J., Vestrand T. W., Wozniak P., Davis H., 2013, ATel, 5316, 1
Zwitter T., Munari U., 2000, Asiago Monografie, Vol. 1, An Introduction to Analysis of Single Dispersion Spectra with IRAF. Osservatori Astronomici di Padova e Asiago, Padova, Italy

SUPPORTING INFORMATION

Supplementary data are available at *MNRAS* online.

suppl data

Please note: Oxford University Press is not responsible for the content or functionality of any supporting materials supplied by the authors. Any queries (other than missing material) should be directed to the corresponding author for the article.

APPENDIX A: SUPPLEMENTARY PLOTS AND TABLES

In this Appendix, we present supplementary plots and tables.

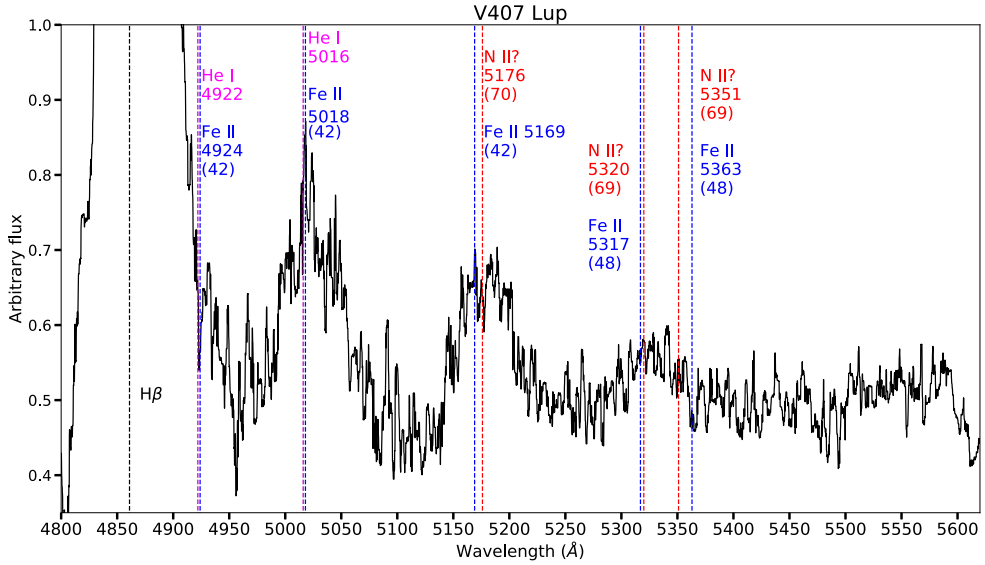

Figure A1. A zoom-in spectral plot of nova V407 Lup on day 6, focusing on the region of Fe II (42) and (48) multiplets.

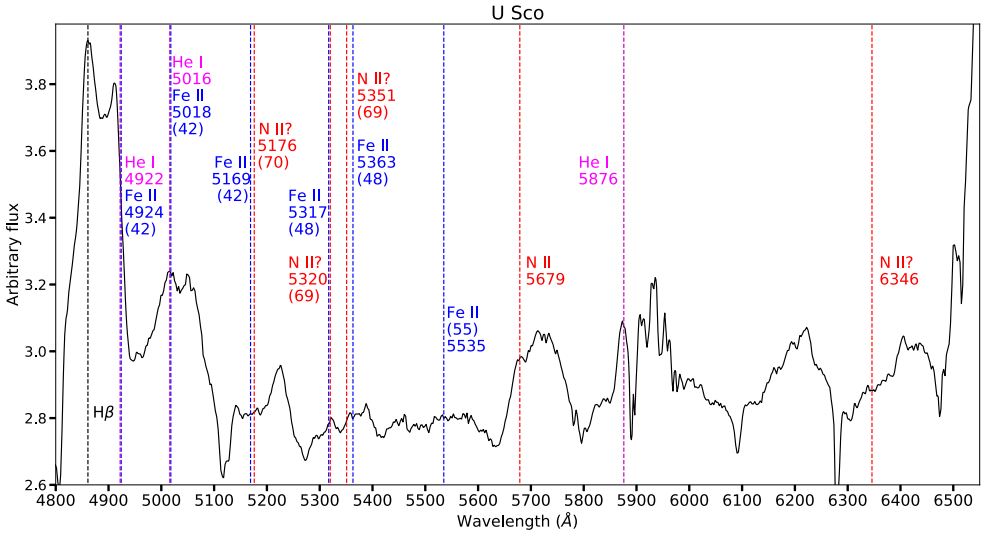

Figure A2. A zoom-in spectral plot of nova U Sco on day 0.7, focusing on the region of Fe II (42) and (48) multiplets, and other He I and N II lines.

Table A1. Spectroscopic observation logs of nova T Pyx (2011).

Source	Date	$t - t_0$ (days)	Resolving power	λ Range (Å)
Astrourf	2011-04-15.8	1.6	1000	3850–6850
Astrourf	2011-04-16.8	2.6	1000	3850–9000
Astrourf	2011-04-17.8	3.6	1000	3850–6850
Astrourf	2011-04-18.8	4.6	1000	3850–6850
Astrourf	2011-04-19.8	5.6	1000	3850–6850
Astrourf	2011-04-21.8	7.6	600	4200–7500
Astrourf	2011-04-29.8	15.6	1000	3850–6850
SMARTS/CHIRON	2011-05-02.2	18	27 000	3800–9530
SMARTS/CHIRON	2011-05-15.2	31	27 000	3800–9530
SMARTS/CHIRON	2011-06-01.2	48	27 000	3800–9530
SMARTS/CHIRON	2011-06-10.2	57	27 000	3800–9530
SMARTS/CHIRON	2011-06-25.2	73	27 000	3800–9530
SMARTS/CHIRON	2011-07-01.2	79	27 000	3800–9530
SMARTS/CHIRON	2011-09-24.2	164	27 000	3800–9530

Table A2. Spectroscopic observation logs of nova V339 Del.

Source	Date	$t - t_0$ (days)	Resolving power	λ Range (Å)
ARAS	2013-08-14.8	0.5	10 000	4200–7300
ARAS	2013-08-15.8	1.5	10 000	4200–7300
ARAS	2013-08-16.8	2.5	10 000	4200–7300
ARAS	2013-08-18.8	4.5	10 000	4200–7300
ARAS	2013-08-19.8	5.5	10 000	4200–7300
ARAS	2013-08-21.8	8.5	10 000	4200–7300
ARAS	2013-08-26.8	13.5	10 000	4200–7300
ARAS	2013-09-01.8	19.5	10 000	4200–7300
ARAS	2013-09-09.8	27.5	10 000	4200–7300
ARAS	2013-09-15.8	33.5	10 000	4200–7300
ARAS	2013-09-21.8	39.5	10 000	4200–7300
ARAS	2013-09-30.8	48.5	10 000	4200–7300
ARAS	2013-10-07.8	55.5	10 000	4200–7300
ARAS	2013-12-01.8	110.5	10 000	4200–7300

Table A3. Spectroscopic observation logs of nova V659 Sct (ASASSN-19aad).

Source	Date	$t - t_0$ (days)	Resolving power	λ Range (Å)
ARAS	2019 Oct 30	1.0	1000	3850–7250
SOAR/Goodman	2019 Nov 03	4	1100	3850–7800
SAOR/Goodman	2019 Nov 04	5	1100	3850–7800
SOAR/Goodman	2019 Nov 05	6	1100	3850–7800
ARAS	2019 Nov 08	9	1000	3850–7250
ARAS	2019 Nov 18	19	1000	3850–7250
SALT/HRS	2020 June 21	236	14 000	4000–8800
SALT/HRS	2020 July 01	246	14 000	4000–8800
SALT/HRS	2020 July 07	252	14 000	4000–8800

Table A4. Spectroscopic observation logs of nova V1405 Cas.

Source	Date	$t - t_0$ (days)	Resolving power	λ Range (Å)
ARAS	2021 Mar 19	1	1500	3900–7300
ARAS	2021 Mar 27	9	14 000	4000–7400
ARAS	2021 Apr 06	19	14 000	3900–7500
ARAS	2021 Apr 19	32	1100	3900–7500
ARAS	2021 May 20	63	1100	3800–7500
ARAS	2021 June 23	97	1100	3800–7500
ARAS	2021 July 11	115	1000	3800–7500
ARAS	2021 July 30	134	1100	3800–7500
ARAS	2021 Aug 16	151	1000	3900–7300
ARAS	2021 Aug 26	161	14 000	3800–7800
ARAS	2021 Sep 10	176	14 000	3800–8900
ARAS	2021 Sep 27	193	1100	3900–7300
ARAS	2021 Oct 04	200	1100	3800–8900
ARAS	2021 Oct 16	212	1100	3800–8900
ARAS	2021 Nov 09	236	1500	3900–7800
ARAS	2021 Dec 22	279	1100	3800–7200
ARAS	2022 Feb 19	338	1100	3800–7500
ARAS	2022 Mar 14	361	1100	3900–7400

Table A5. Spectroscopic observation logs of nova V606 Vul.

Source	Date	$t - t_0$ (days)	Resolving power	λ Range (Å)
Asiago	2021-07-17.12	1.8	TBA	3850–7750
Asiago	2021-07-18.8	3.5	TBA	3800–7300
Asiago	2021-07-19.8	4.5	TBA	3850–7750
ARAS	2021-07-21.5	6	1000	4000–7500
ARAS	2021-07-24.5	9	1000	4000–7500
ARAS	2021-07-26.5	11	1000	4000–7500
ARAS	2021-07-27.5	12	1000	4000–7500
Asiago	2021-07-28.8	13.5	TBA	3800–7300
ARAS	2021-07-30.5	15	1000	4000–7500
SOAR	2021-07-30.5	15	1000	800–7500
ARAS	2021-08-06.7	22.4	1000	3800–7400
Asiago	2021-08-18.8	33.5	TBA	3850–7750
ARAS	2021-08-25.5	41	1000	4000–7500
ARAS	2021-09-04.5	51	1000	4000–7500
ARAS	2021-10-25.5	101	1000	4000–7500
ARAS	2021-11-01.5	109	1000	4000–7500
ARAS	2021-11-06.5	114	1000	4000–7500
ARAS	2021-11-10.5	118	1000	4000–7500
ARAS	2021-11-12.5	120	1000	4000–7500
ARAS	2022-03-25.5	253	1000	4000–7500
Asiago	2022-11-07.8	480	TBA	3850–7750

Table A6. Spectroscopic observation logs of nova *Gaia*22alz.

Source	Date	$t - t_0$ (days)	Resolving power	λ Range (Å)
SALT/RSS	2022 Mar 10	45	1500	4200–7300
SALT/HRS	2022 Mar 15	49	14 000	4000–9000
SALT/HRS	2022 Apr 03	68	14 000	4000–9000
SOAR/Goodman	2022 Apr 09	76	1100	3800–7800
SOAR/Goodman	2022 Apr 14	80	1100	3800–7800
SOAR/Goodman	2022 Apr 21	86	1100	3800–7800
ARAS	2022 Apr 30	95	1000	4000–7800
SOAR/Goodman	2022 May 01	96	1100	3800–7800
ARAS	2022 May 02	97	1000	4000–7800
SALT/HRS	2022 May 08	103	14 000	4000–9000
SALT/HRS	2022 May 11	106	14 000	4000–9000
SOAR/Goodman	2022 May 22	118	1100	3800–7800
SOAR/Goodman	2022 May 24	120	1100	3800–7800
SOAR/Goodman	2022 June 09	135	1100	3800–7800
Magellan/IMACS	2022 July 21	178	1500	3800–6600
SOAR/Goodman	2022 Aug 15	203	1100	3800–7800
SOAR/Goodman	2022 Aug 24	212	1100	3800–7800
SOAR/Goodman	2022 Sep 17	236	1100	3800–7800
SOAR/Goodman	2022 Oct 08	257	1100	3800–7800
SOAR/Goodman	2022 Oct 18	267	1100	3800–7800
SOAR/Goodman	2022 Oct 29	278	1100	3800–7800
SOAR/Goodman	2022 Dec 01	310	1100	3800–7800
SOAR/Goodman	2023 Jan 20	360	1100	3800–7800
SOAR/Goodman	2023 Feb 28	399	1100	3800–7800
SOAR/Goodman	2023 Mar 15	414	1100	3800–7800
SOAR/Goodman	2023 Mar 25	424	1100	3800–7800
SOAR/Goodman	2023 Apr 04	434	1100	3800–7800
SOAR/Goodman	2023 June 06	497	1100	3800–7800

Table A7. Spectroscopic observation logs of nova V612 Sct.

Source	Date	$t - t_0$ (days)	Resolving power	λ Range (Å)
Asiago	2017 June 25	6	TBA	4000–7800
ARAS	2017 June 29	10	1000	4400–7400
ARAS	2017 June 30	11	1000	4400–7400
ARAS	2017 July 02	12	1000	4400–7400
ARAS	2017 July 06	16	1000	4400–7400
ARAS	2017 July 07	17	1000	4400–7400

Table A8. Spectroscopic observation logs of nova FM Cir.

Source	Date	$t - t_0$ (days)	Resolving power	λ Range (Å)
SMARTS/CHIRON	2018-01-20.5	2.8	27 000	4100–8900
SMARTS/CHIRON	2018-01-22.5	4.8	27 000	4100–8900
SMARTS/CHIRON	2018-01-23.5	5.8	27 000	4100–8900
SMARTS/CHIRON	2018-01-25.5	7.8	78 000	4100–8900
SMARTS/CHIRON	2018-01-31.5	13.8	78 000	4100–8900

Table A9. Spectroscopic observation logs of nova V407 Lup.

Source	Date	$t - t_0$ (days)	Resolving power	λ Range (Å)
ARAS	2016-09-24.5	0.5	1000	4200–7300
VLT-Pucheros	2016-09-29.5	5.5	20 000	4250–6900
VLT-UVES	2016-10-02.5	8.5	59 000	3060–9460
ARAS	2016-10-04.5	10.5	1000	4200–7300
VLT-UVES	2016-10-12.5	18.5	59 000	3060–9460

Table A10. Spectroscopic observation logs of nova U Sco (2022).

Source	Date	$t - t_0$ (days)	Resolving power	λ Range (Å)
SALT/HRS	2022-06-07.0	0.3	14 000	4000–8800
ARAS	2022-06-07.2	0.5	1000	3800–7200
ARAS	2022-06-07.4	0.7	1000	3800–7200
ARAS	2022-06-07.8	1.1	1000	3800–7200
ARAS	2022-06-08.3	1.6	1000	3800–7200

[1]*Department of Physics and Astronomy, Center for Data Intensive and Time Domain Astronomy, Michigan State University, East Lansing, MI 48824, USA*
[2]*Department of Astronomy, University of Illinois at Urbana-Champaign, 1002 W. Green Street, Urbana, IL 61801, USA*
[3]*Sternberg Astronomical Institute, Moscow State University, Universitetskii pr. 13, 119992 Moscow, Russia*
[4]*Department of Astronomy & Astrophysics, University of California, 1156 High St, Santa Cruz, CA 95064, USA*
[5]*Space Telescope Science Institute, 3700 San Martin Drive, Baltimore, MD 21218, USA*
[6]*South African Astronomical Observatory, P. O. Box 9, 7935 Observatory, South Africa*
[7]*Department of Astronomy, University of Cape Town, Private Bag X3, Rondebosch 7701, South Africa*
[8]*Centro de Estudios de Física del Cosmos de Aragón, Plaza San Juan 1, E-44001, Teruel, Spain*
[9]*UK Astronomy Technology Centre, Royal Observatory, Blackford Hill, Edinburgh, EH9 3HJ, UK*
[10]*DARK, Niels Bohr Institute, University of Copenhagen, Jagtvej 128, DK-2200 Copenhagen Ø, Denmark*
[11]*National Radio Astronomy Observatory, P. O. Box O, Socorro, NM 87801, USA*
[12]*Southern African Large Telescope Foundation, P. O. Box 9, Observatory 7935, South Africa*
[13]*Special Astrophysical Observatory, Nizhnij Arkhyz, Karachai-Circassia 369167, Russia*
[14]*Department of Physics and Columbia Astrophysics Laboratory, Columbia University, New York, NY 10027, USA*
[15]*Center for Computational Astrophysics, Flatiron Institute, 162 5th Avenue, New York, NY 10010, USA*
[16]*Nicolaus Copernicus Astronomical Center, Polish Academy of Sciences, Bartycka 18, PL 00-716 Warsaw, Poland*
[17]*INAF – Osservatorio Astronomico di Trieste, Via G. B. Tiepolo 11, I-34143 Trieste TS, Italy*
[18]*Institute of Fundamental Physics of the Universe, Via Beirut, 2, I-34151 Trieste TS, Italy*
[19]*CRESST and X-ray Astrophysics Laboratory, NASA/GSFC, Greenbelt, MD 20771, USA*
[20]*Department of Physics, University of Maryland, Baltimore County, 1000 Hilltop Circle, Baltimore, MD 21250, USA*
[21]*INAF Astronomical Observatory of Padova, I-36012 Asiago (VI), Italy*
[22]*INAF – Osservatorio di Padova, vicolo dell'Osservatorio 5, I-35122 Padova, Italy*
[23]*Department of Astronomy, University of Wisconsin, 475 N. Charter St., Madison, WI 53704, USA*
[24]*Department of Physics, Center for Materials Research, Norfolk State University, Norfolk, VA 23504, USA*
[25]*Institute for Astronomy, University of Hawai'i, 2680 Woodlawn Drive, Honolulu, HI 96822, USA*
[26]*Department of Astronomy and Theoretical Astrophysics Center, University of California, Berkeley, CA 94720, USA*
[27]*Columbia Astrophysics Laboratory and Department of Physics, Columbia University, New York, NY 10027, USA*
[28]*Department of Physics & Astronomy, Stony Brook University, Stony Brook, NY 11794-3800, USA*

This paper has been typeset from a TEX/LATEX file prepared by the author.